LATE NEOGENE AND QUATERNARY STRATIGRAPHY AND STRUCTURE OF LITTLE LAKE VALLEY, NORTHERN COAST RANGE, CALIFORNIA

by

Adam C. Woolace

A Thesis

Presented to

The Faculty of Humboldt State University

In Partial Fulfillment

Of the Requirements for the Degree

Master of Science

In Environmental Systems: Geology

May, 2005

ABSTRACT

LATE NEOGENE AND QUATERNARY STRATIGRAPHY AND STRUCTURE OF LITTLE LAKE VALLEY, NORTHERN COAST RANGE, CALIFORNIA

Adam Woolace

Little Lake Valley is an intermontane basin within the northern California Coast Ranges that contains a record of Pleistocene basin sedimentation and deformation. Valley fill, estimated at up to 1100 m thick, tilts uniformly to the north with a mean dip of ca. 8° and a range of 5° to 25°. Northward tilt and subsidence is accommodated along two fault strands that are now inactive, the East Valley fault and the North Valley fault. Tephra located in the sediment fill have Pleistocene ages: The Thermal Canyon ash (740 ka), the Rockland ash (~575 ka) and an unnamed tephra correlative to tephra in the Clear Lake basin (~110 ka). Maximum age of basement fill is estimated at ~1.2 My. Locations of known tephra were used to calculate a valley sedimentation rate of ~1.1 m/thousand years. Based on offset tephra, the slip rate of the right lateral Maacama fault is estimated at ~5 mm/yr since ~0.75 Ma. Paleoflow direction, for basement sediment, as determined from clast imbrication and channel margin trends, is to the south; in contrast, surface drainage on the valley floor is presently to the north. Facies relations inferred from well logs indicate that streams aggrading the valley were through-going streams traveling south along the valley axis. A depositional facies transition occurs during the late Pleistocene from high energy streams with coarse bed load to lower energy, fine grained streams. Northward tilt during the latest Pleistocene led to river capture and drainage reversal in LLV. The northward tilt of basin strata is part of a regional extensional response to the northward passage of the Mendocino triple junction.

ACKNOWLEDGMENTS

I would like to extend the utmost appreciation to the following committee members: Harvey Kelsey, Gary Simpson, Bob McLaughlin, and Kevin Furlong, their guidance has been invaluable. I also want to thank Amy Thomson for her support, advice, patience, and love. Appreciated both in the field and in the office was the assistance of John Wellik, Mort Larsen, Todd Williams, Jay Patton and Michelle Roberts. I will always be extremely grateful to Andrei Sarna-Wojicicki for his wonderful generosity and guidance. I also extend my gratitude to Tor Nilsen and Carol Prentice, for their accompaniment in the field. The California Department of Water Resources (CDWR), also contributed to the completion of this manuscript, and for that I am thankful. Most importantly I would like to thank my parents Larry and Donna, and my sisters Rachel and Elizabeth for their continuous support, understanding, and love.

TABLE OF CONTENTS

TABLE OF CONTENTS, CONTINUED

LIST OF TABLES

LIST OF FIGURES

INTRODUCTION

Little Lake Valley (LLV) lies approximately 60 km east of the Pacific Ocean in the Coast Range of northern California. Basement rock beneath and surrounding LLV consists of Jurassic and Cretaceous age Central Belt Franciscan (Jennings and Strand, 1960). The area lies within the strike-slip deformation boundary zone between the North American and Pacific Plates (Figure 1). The purposes of this study are to gain an understanding of the Pliocene and Quaternary stratigraphic record and tectonic evolution of Little Lake Valley, to gain insight into the geomorphic response of the LLV region to the migrating Mendocino Triple Junction, and to understand the timing of initiation of slip on the Maacama fault relative to the timing of basin formation.

PREVIOUS WORK

In 1956, the California Department of Water Resources (CDWR) conducted the first significant geologic study of LLV as part of an investigation of aquifers located in alluviated valleys throughout northwestern California. Nine years later Cardwell (1965) conducted a more in-depth study that focused on stratigraphic relations (from well logs) and groundwater characteristics in several valleys including Little Lake Valley. On the basis of well logs, Cardwell (1965) inferred fluvial and lacustrine deposits are widespread in both Little Lake Valley and Upper Russian River Valley. Based on sub-surface bedrock geometry, Cardwell (1965) speculated that sedimentary units in Little Lake Valley are as much as 500 m thick in the southwestern part of the valley, disregarding the possibility of structural discontinuities. However, the deepest drill boring in sediment is this study is 160 m. Both CDWR (1956) and Cardwell (1965) speculate the age of the basin fill to be Pliocene to Pleistocene in age on the basis of a comparison to similar alluviated deposits in alluvial valleys to the south near Santa Rosa, but neither CDWR (1956) nor Cardwell (1965) offer data to support their age speculations. The Rockland ash was identified within sedimentary fill in the southern end of Little Lake Valley about 3.5 km south-southeast of the town of Willits, CA (Sarna-Wojcicki et al., 1985 and Meyer et al., 1991). The age of the Rockland ash is estimated to be 575 ka (Lanphere et al., 1999).

Bedrock lithology of the Coast Range surrounding Little Lake Valley consists of Jurassic and Cretaceous Central Belt Franciscan sandstone, greywacke, mudstone, and shale with less abundant stringers containing greenstone, blueschist, and serpentine (Jennings and Strand, 1960). The predominant Franciscan units surrounding Little Lake Valley are sedimentary marine rocks containing bodies of chert and greenstone. Throughout the area bedrock is extensively sheared and fractured (Cardwell, 1965).

Northward migration of the Mendocino Triple Junction (MTJ) (Figure 1) has played a fundamental role in the tectonic evolution of LLV. The MTJ originated approximately 30 Ma when the Pacific-Farallon ridge system first collided with the North American plate (Atwater, 1970). The result of this collision was the formation of two triple junctions. The northerly (Mendocino Triple Junction) moved to its present day location at Cape Mendocino, as the southerly (Rivera Triple Junction) moved south to its present position in the Gulf of California.

The migrating MTJ produces uplift (that leads to the emergence of the coast and formation of the Coast Range) and induces volcanism within the range. The recent emergence of the coast near Cape Mendocino coincides with the location of the MTJ region (Merritts and Bull, 1989). As the MTJ migrates north, crustal thinning occurs in the wake of the subducted Gorda plate (Furlong and Govers, 1999). Crustal processes within the "slab window" (Furlong and Govers, 1999; Furlong et al., 2003; Furlong and Schwartz, 2004) result in a chain of volcanoes that young to the north (Fox et al., 1985). The ages of these volcanic rocks suggest that volcanism in the Northern Coast Range migrated northwestward at a rate of ~3.75 cm/yr from 25 to 12 Ma, and ~1.3 cm/yr from 12 Ma to present (Fox et al. 1985). This is equivalent to the rate of MTJ migration, assuming the MTJ migrates at the velocity of the Pacific plate relative to North America and that a slab window develops in the wake of migration (Furlong and Schwartz, 2004).

Neogene age structural basins of the northern Coast Ranges provide evidence of extension that can be attributed to the northward propagation of the San Andreas transform margin. The northern San Andreas right-lateral strike-slip system covers a broad 80-90 km wide zone that extends from San Francisco north to Cape Mendocino. Transform motion is accommodated by several major fault zones including the San Andreas, Healdsburg-Rogers Creek, Maacama, Green Valley and Bartlett Springs (Figure 1). Few studies have documented the kinematics of Coast Range basins, but Dickinson and Snyder (1979) suggested that the origin of intermontane basins of the Coast Range, such as Ukiah Valley, Round Valley, and LLV, may be related to the San Andreas fault system. McLaughlin and Nilsen (1982) studied the Little Sulphur Creek basins southeast of Ukiah (Figure 1), and proposed that these basins formed as right-lateral strike-slip pull-apart basins along the Maacama fault.

The Maacama fault is an active strike-slip fault that accommodates transform motion along the Pacific-North American plate boundary (Figures 1 and 2). The Maacama fault is a continuation of several faults including the Hayward, Rodgers Creek and Healdsburg faults. As the Maacama fault propagated northward in the wake of the northward-migrating Mendocino Triple Junction, a strike slip tectonic regime replaced fold and thrust belt tectonics of the pre-existing convergent North American plate margin (Kelsey and Carver, 1988). Several studies have documented crustal deformation associated with the Maacama fault zone. Pampeyan et al. (1981) and Upp (1989) mapped active traces of the Maacama fault zone. The northern Maacama fault extends north a distance of more than 100 km from the Mendocino County/Sonoma County line to north of Laytonville, and traverses the southwestern corner of Little Lake Valley through the city of Willits (Upp, 1989) (Figure 3). The fault zone has an overall trend of N27°W, although individual fault segments trend from N8°W to N47°W (Upp, 1989) (Figure 2). The Willits fault, mapped by Upp (1989), occupies the eastern margin of LLV. We have reevaluated the Willits fault and renamed it the East Valley fault on the basis of that the fault does not pass through the city of Willits.

Geodetic and geologic studies on the northern Maacama fault provide several estimates of slip rate. Freymueller et al. (1999) published horizontal slip-rates on the Maacama fault near Garberville, California as high as 13.9 mm/yr based on global positioning system (GPS) geodetic measurements taken over a four-year period. This estimate is considerably higher than estimated rates of near-field shallow creep along the fault (Galehouse, 2002) suggesting that the shallow creep only relieves a fraction of the stress (Freymueller et al., 1999). Galehouse (2002), who conducted a creep rate study on the Maacama fault in Willits, CA using theodolite measurements, measured a creep rate of 6.6 mm/yr over a nine-year period. McLaughlin (2000, 1981) calculates a ~5 mm/yr slip rate on the southern Maacama fault based on 20 km of right lateral offset of 2.5-6.0 My Sonoma volcanic rocks.

Various studies have predicted the seismic potential and earthquake recurrence interval of the Maacama fault. Based on paleoseismic trench investigations in Little Lake Valley, Upp (1989) concludes at least two and probably three surface rupture events have occurred within the past 16,200 years along the Maacama fault in Little Lake Valley. Fenton et al. (2002) conducted a series of paleoseismic trench excavations in Little Lake Valley in order to determine slip-rate and recurrence interval data. The study concludes that up to five significant earthquakes have occurred in the late Holocene (Fenton et al., 2002).

RESEARCH APPROACH

Investigation of the sedimentary history of LLV involved several strategies: field mapping of road cut, stream cut and railroad cut exposures, compilation of well logs and observations from trench excavations within the valley where trenches were open for geotechnical or paleoseismic investigation. Geotechnical and paleoseismic trenches provided sediment samples for age determination and provided opportunities to document the nature of the upper ~ 9 m of valley fill deposits.

The combined results of the field mapping (Figure 3) and well log compilation (Figures 4, 5, 6 and 7) give a picture of the sediment type and geometry of sedimentary units. The well log data also provided an opportunity to view the three-dimensional geometry of the sedimentary units, from which depositional systems and facies models are inferred. The well log data also allowed evaluation of whether any of the basin margins were fault controlled. Surface outcrops, mainly in the southern part of LLV, provided data on paleo flow direction and post-depositional tilting of the sediment.

AGE DATA FOR SEDIMENT WITHIN LITTLE LAKE VALLEY

The youngest sediment in the LLV is latest Holocene because LLV is an actively aggrading sedimentary basin. The oldest sediment in the LLV basin is constrained to be younger than the age of the basement rocks that underlie the basin, which consist of the Mesozoic Franciscan Formation. The oldest basin sediment, directly above the Franciscan contact, is nowhere exposed in the basin and has not been dated.

Radiocarbon ages on organic material within the upper 9 m of basin sediment provide a measure of the depth of Holocene sediment in the southern part of LLV (Figure 8). Two radiocarbon samples, one from the wall of a geotechnical trench (Figure 8A, site 'X') and the other from an exposure on the floor of Haehl Creek (Figure 8A, site 'Y'), are latest Pleistocene in age (Table 1, Figure 8). These latest Pleistocene ages establish that overlying unconsolidated alluvial strata in the upper 5-7 m of the southern part of the valley are Holocene in age. At Site Y (Figure 8), carbonized seeds were collected from an organic-rich silt bed exposed near the active channel of Haehl Creek. The bedding orientation of the unit is N10°W, 4° NE. The seeds were identified by Jim Effenberger, of California Department of Food and Agriculture Seed Laboratory as probably Fabaceae *Lupinus*, or lupine, which is a native species common to low-lying damp locations throughout the northern Coast Ranges. The calibrated ^{14}C age of the seeds is 17,813-19,974 Cal yr B.P. (Table 1). Nearly 200 m due east the of seed location in a geotechnical trench on the alluvial plain of Haehl Creek (Figure 8A, site 'X'), a 4 cm piece of root from a tree buried by 8 m of alluvium was collected for ^{14}C analysis (Figure 8, Table 1). The tree was in growth position although it appeared to have died and weathered sub-aerially before being buried; the tree trunk had no bark yet bark was well preserved on the roots. The calibrated age of the root is 13,422-13,543 Cal yr B.P. (Table 1). Date from root is consistent with other dates from trees and charcoal from both geotechnical and research trench studies conducted near Haehl Creek (Fenton et al., 2002; Gary Simpson, pers. comm., 2005).

Tephrochronology provides several important ages for Pleistocene sediment in southern LLV (Table 2). Under the supervision of Andrei Sarna-Wojcicki of the U. S. Geological Survey's Tephrochronology Laboratory, several tephra found in LLV sediment were analyzed and correlated to known tephra sources. Thermal Canyon tephra (740 ka) occurs in a lignite unit in a Haehl Creek stream cut (Figure 8A, site 'T'). The tephra is slightly disturbed and discontinuous with a bedding orientation of N 30° W, 14° NE. The Rockland ash (~575 ka) located previously in a road-cut east of Highway 101 at the southern end of the valley (Figure 8) (Sarna-Wojcicki et al., 1985; Meyer et al., 1991; Lanphere et al., 1999). An unnamed tephra was recovered from a geotechnical excavation on the Maacama fault in the city of Willits (Figure 8A, site 'S'). The tephra was located directly in the fault zone, within distinct, well-bedded yet laterally discontinuous (faulted) strata (Gary Simpson, pers. comm. Sept. 2003). The unnamed tephra geochemically correlates to a tephra identified in a core from Clear Lake that has a sedimentation rate-estimated age of ~110 ka (Sarna-Wojcicki et al., 1988).

DESCRIPTION OF BASIN GEOMETRY AND SEDIMENTARY HISTORY

Stratigraphic and Structural Data from Well Logs

Well logs that are archived with the California Department of Water Resources (CDWR) provide stratigraphic and structural data on LLV sediment and basin geometry. Since the 1940's, California state law has required well drillers to complete detailed well logs at drill sites. (CDWR) provides limited access to well logs for educational and scientific purposes, and I was granted access to well logs pertaining to my field area at the CDWR headquarters in Sacramento, CA. Well logs include general descriptions of stratigraphic units based on texture, depth to contacts, depth to water table, and flow capacity of aquifer. Although well logs provide stratigraphic data, caution must be taken when using them for geologic interpretation because descriptions and the level of accuracy vary among logs.

The first step in using well logs is to determine the location of each significant well. Most logs are referenced to an address and/or an assessor parcel number (APN). Well logs with addresses were located using "mapquest.com". Well logs with an APN were located using APN maps from Mendocino County Tax Assessor. Individual wells that could not be located accurately were discarded.

Sixty-four wells were located within LLV, and along the immediate fringe (Figure 4). Wells tend to be clustered in populated portions of the valley (There is a significant gap in the northern part of the valley), but there is broad distribution across the valley. Locations were selected on the basis of locations of clusters of significant well logs.

Topography was appended to both ends of the transect in order to depict the topographic cross-section of the valley (Figure 5, 6 and 7). Wells not positioned directly on a transect line were projected perpendicularly to the line and data were then plotted on the transect (Figure 4). Well log descriptions of geologic units are typically classified based on texture and color and include: loam, gravel and boulders, clay with gravel, sand, sandy clay, blue clay, yellow clay, brown clay, tephra, and Franciscan bedrock.

Subsurface Basin Geometry

Well logs provide insight into the subsurface geometry of the LLV basin. As mentioned earlier, the maximum depth of bedrock in LLV in unknown. Cardwell (1965) predicts the basin sediment to be as much as 500 m thick but provides no data to support his hypothesis. Because of the considerable thickness of the valley fill, well logs other than those on or near the flanks of the valley do not penetrate to bedrock. The deepest well log in the valley is 160 m. Well A2 (160 m) and well A1 (107 m) are both located near the center of the valley (Figure 6), and do not reach bedrock. On the northern and eastern valley margins, well logs illustrate abrupt changes in depth to bedrock, suggesting steep or sometimes precipitous, valley margins. For instance, well logs on transects B-B' and C-C' show an abrupt increase in bedrock depth (Figures 5 and 6). I propose the steep nature of the valley margin on the eastern side of LLV to be a product of at least 30 m of vertical displacement on an east-side-up fault, which I name the East Valley fault (Figures 3 and 6).

Another fault, referred to herein as the North Valley fault (Figure 3), is inferred from well log-derived depth to Franciscan bedrock in the northern part of the valley. Much like the East Valley fault, adjacent well logs show an abrupt change in depth to basement between the inferred up-thrown block and downthrown block of the proposed North Valley fault. Shallow depth to basement of wells in cross-section A-A' provides evidence that a fault lies between A-A' and cross section B-B', where wells in the middle of the valley do not penetrate basement. In addition, in well log cross-section B-B' (Figure 5) between well log 8 and 9, nearly 15 m of inferred offset is present. The shallow bedrock at the northern end of LLV is referred to by CDWR (1956) as a "bedrock ledge".

Pleistocene and Older Sediment Within Little Lake Valley

Pleistocene alluvium, exposed as uplifted, eroded valley fill, forms the low hills south-southeast of the city of Willits in the southern part of the LLV (Figure 3). Gravel, sand, silt and clay are the main sedimentary units. In the central part of the valley, Pleistocene sediment is buried by Holocene alluvium, found in incised stream banks. In the northern part of the valley Pleistocene sediment is too deeply buried and is not exposed.

Pleistocene strata uniformly tilt down to the north with a mean dip of 8° and a range of 5° to 25° (inset, Figure 3). Bedding measurements are easily obtained in most exposures of Pleistocene sediment; fine grained sediment such as clay and silt tend to produce more consistent bedding orientations than coarser grained sand and gravel. Units with abundant carbon and plant material are highly fissile and make the best candidates for bedding measurements. In the Maacama fault zone, locally steep bedding dips (up to vertical and overturned) are not uncommon; therefore, I discarded measurements found in and near fault zones when compiling the bedding orientations depicted in Figure 3.

Gravel and sand units dominate the Pleistocene section in the low hills in the southern portion of the valley, but these coarse units are interbedded with lenses of clay and silt up to 5 m thick (cross section F-F’, wells 54 and 55, Figure 7). The coarsest clasts exposed in outcrop are boulders up to 60 cm that occur in a railroad cut on the southwest flank of the valley (Figure 9). The railroad cut contains massive, sub-angular to well-rounded, unsorted gravel; the gravel is clast-supported with a sand matrix. In the south-central part of the valley, gravel exposed in low hills consists of clasts ranging from 1 mm to 10 cm with well-developed imbrication. Pebble and cobble clasts are derived from Jurassic and Cretaceous age Central Belt Franciscan graywacke sandstone, mudstone, shale, greenstone, blueschist, and serpentine.

Pleistocene or Older Sediment Northwest of Little Lake Valley

An isolated exposure of Pleistocene or older sediment (‘airport gravels’) occurs northwest of Little Lake Valley on and near the site of Ellis-Willits airport over 200 m above the valley floor at an elevation of 610 m (Figure 3). These deposits consist of highly weathered, well-consolidated fine and coarse grained alluvium. The gravel is matrix supported although the degree of weathering has completely destroyed the fine grained material and only coarse siliceous clasts such as quartz and chert remain. The chert and quartz clasts are well preserved and range from sub-rounded to well-rounded. The measurable clasts range from 1 cm to 15 cm in size. Many ghost clasts are present as well and appear to be of siltstone and sandstone origin.

Holocene Sediment Within Little Lake Valley

Fine and coarse grained unconsolidated alluvium and colluvium of inferred Holocene age constitute most of the exposed sediment that occurs in the 31 km^2 northern two-thirds of the valley (Figure 3). These deposits consist of clay, silt, sand, and gravel and are derived from the erosion of the mountains adjacent to the valley and from the reworking of older sediments in the southern part of the valley. The sediment is transported northward through the basin by several streams including Haehl, Davis, Broaddus, Baechtel, Willits, and Berry Creeks.

The thickness of Inferred Holocene age deposits varies, but in general these recent sediments in LLV thickens to the north. Holocene deposits are absent on the hills south of Willits and are as thin as 1 m in the upper reaches of Haehl Creek. In geotechnical trenches in the southern central part of the valley (site X, Figure 8A), 7.5 m of Holocene Haehl Creek alluvium overlies late Pleistocene clayey silt. Assuming that the upper layer of Holocene sediment is uniformly fine where it occurs in the northern part of the valley, then such sediment is as thick as 30 m where observed in well log cross-sections A-A', B-B', and C-C' (Figures 5 and 6).

An actively aggrading, poorly drained lowland exists in the northern portion of the valley. The poor drainage is likely caused by the bedrock sill at the northern end of the valley, which limits incision and controls base level at the valley's outlet. This bedrock is exposed in the channel bed at the head of Outlet Creek and is the base level for drainage to the north out of Little Lake Valley. In the early 20th century, the poorly drained northern portion of Little Lake Valley was a much more extensive shallow lake. Human excavations have increased the depth of Outlet Creek in order to decrease the extent of the shallow lake, allowing more water and sediment to escape (Rod Dockins, pers. comm. 2002; B. Garman, pers. comm. 2003.).

Landslides contribute Holocene colluvium to the valley sediment fill. Most landslides are on the northern and eastern sides of the valley (Figure 3) and erode hillslopes on the upthrown sides of the inferred East Valley and North Valley faults. One such landslide is evident in well log cross-section A-A' (Figure 5) where well logs 70A, 76, 77, and 80 contain 10-20 m of coarse gravel that I infer is coarse colluvium derived from a large landslide on the adjacent uplands depicted on the geologic map at the far northern end of the valley. Smaller landslides are mapped on the eastern flank of the valley, at the mouth of Outlet Creek, and at the northwestern end of the valley (Figure 3).

BASIN PALEOFLOW DIRECTION

Imbrication measurements taken in Little Lake Valley indicate a general paleo sediment transport direction to the south-southeast, parallel to the longitudinal axis of the valley. 295 paleo-current measurements were taken on imbricated clasts at various Pleistocene gravel outcrops (Figure 11). The orientation of the planes of geometrically planar clasts was measured with a pocket transit. To maintain consistency, I made all of the measurements while an assistant recorded the measurements. In some cases the use of a shovel or a pick was used to expose clasts; excessive digging that could disturb clasts was avoided. Each clast was removed after measuring to ensure that the clast was planar and to avoid repeated measurements on the same clast. A poles to planes stereonet plot was then developed on a great circle and rose diagrams were created using the program *Stereowin* (fttp://www.geo.cornell.edu/pub/rwa/Windows/StereoWinFull120.zip). Because Little Lake Valley has a mean regional bedding dip of 8^o to the north, the data were rotated south in order to depict flow direction on the basis of untilted alluvium. Clast imbrication was measured at five sites (A, B, C, D and E, Figure 11) and each site contained a minimum of 40 measurements. The sample area of each site was no larger than 4 m^2, and each location was chosen because it had planar, imbricated clasts. Well sorted and rounded gravel provides more consistent data than poorly sorted angular gravel. Site B combined data from two separate outcrops approximately 8 m apart. Site C combined data from opposite sides of a road.

Site B, a deep railroad cut on the southeastern margin of the valley (Figure 11), contains coarse, well-preserved, moderately rounded, moderately sorted, clast supported gravel, with clasts ranging from 2 cm to 50 cm (Figure 9). The railroad cut optimizes the opportunity to measure in-place clasts.

Data from sample site C were taken from well-rounded, clast supported, moderately sorted, coarse gravel (5-40 mm) that overlies a 2 m thick sandy-silt unit. Site C gravel generally fines upward with massive basal channel conglomerate underlying cross stratified sandstone. The orientations of cross-bedding and channel margin trends suggest southeast oriented channels (T.H. Nilsen, pers. comm. Aug 4, 2003).

Site A contains subrounded, matrix supported sediment ranging from sand to boulders. The site is poorly preserved and highly weathered with siliceous clasts such as greenstone, chert and quartz being well preserved while non-siliceous mudstone and shale are highly weathered. The outcrop is an actively eroding road cut and may contain disturbed sediment. Paleoflow data is of questionable quality because of poor preservation, possible post-depositional movement, and a sedimentary environment not conducive to clast imbrication.

Site E contains coarse, matrix supported, poorly sorted sand, gravel and boulders. Siliceous clasts are well preserved but much of the mudstone/sandstone matrix and the non-siliceous gravels are highly weathered.

In all sites the mean vector direction on the rose diagram (Figure 11) suggests paleoflow direction to the southeast. Sites B, C and D, which contain the tightest data array, have pole-to-plane trends ranging from 141^{o} to 169^{o} with dips ranging from 64^{o} to 73^{o} toward the south. Sites B, C, and D indicate a sediment transport direction to the south-southeast. At sites A and E, the poles to planes stereo plots have a broader range. The mean vector direction of site A is 222^{o} with 69^{o} dip to the south; mean flow direction is to the southwest. Site E contains the most data spread with a mean trend and plunge for poles to planes of 186^{o} and a dip of 86^{o} south.

In conclusion, I infer on the basis of imbrication data as well as field observations of channel margin trends that Pleistocene paleoflow (transport direction was to the SSE, roughly parallel to the long-axis of the valley. At-a-site variability of paleoflow data is the result of several variables: clast geometry, depositional facies, quality and extent of clast sorting, and preservation of outcrop. The clast geometry at a particular outcrop determines the consistency of paleo current data. Sites with an abundance of clasts with linear and planar geometry produce tighter data (sites B, C and D) than sites lacking such features (A and E). Well-sorted sediment and sediment with clast-supported matrix also minimize data spread.

DISCUSSION

Sedimentation Rate in LLV Inferred From Tephrochronology

The presence of three identified tephra deposits in LLV stratigraphy provides the opportunity to estimate the duration of sedimentation in LLV and to calculate an approximate basin sedimentation rate for a 465,000 to 630,000-year time period from the time of deposition of the mid Pleistocene tephras (Rockland, 575 ka; Thermal Canyon, 740 ka) to the time of deposition of the youngest tephra (Unnamed, 110 ka). However, because the 0.11 Ma tephra (site S, Figure 8A) could be located either on the eastern or western side of the Maacama fault, two sedimentation rates were calculated using the two alternative interpretations. If the 110 ka tephra is to the west of the fault, it is on the same side of the fault as the Thermal Canyon tephra (740 ka), yielding a map distance separation of 2,130 m over a time span of 630 ky. Accounting for an 8°N regional dip, the true thickness of the section is 296 m and the sedimentation rate is 0.47 m/ky (Figure 12). Alternatively, the unnamed tephra may be on the eastern side of the Maacama fault and on the same side of the fault as the Rockland tephra (575 ka), yielding a map distance separation of 3,800 m over a time span (575 ka minus 110 ka) of 465 ky. Accounting for the 8°N regional dip, the true thickness of the section is 530 m and the sedimentation rate over 465 ky is ~1.1 m/ky.

Knowing an estimate of the minimum thickness of the Pleistocene section in LLV, we can assess which of the two sedimentation rate estimates is more consistent with the observation that the Thermal Canyon tephra (740 ka) is in the lower half of the

Pleistocene section (Figure 13). The minimum thickness of the Pleistocene fill in LLV, on the basis of regional bedding tilt, exposed outcrops at the southern end of the valley, and minimum thickness from well logs, is on the order of 1,100 m (Figure 13). If the sedimentation rate is 0.4 m/ky, then 1,000-1,200 m of fill would have been deposited in 2.5 to 3.0 My, which is inconsistent with the Thermal Canyon tephra (740 ka) being in the lower half of the Pleistocene section. If the sedimentation rate is 1.1 m/ky, then 1,000-1,200 m of fill would have been deposited in 1.1 to 1.3 My. A duration of deposition of 1.1 to 1.3 My is more consistent with the Thermal Canyon tephra (740 ka) being in the lower half of the Pleistocene sedimentary section. Therefore it is more likely that the 0.11 Ma tephra is in unfaulted stratigraphic order with the 740 ka Thermal Canyon tephra on the eastern side of the Maacama fault, and subsequent fault slip rate calculations use the assumption that the 0.11 Ma unnamed tephra is located on the eastern side of the Maacama fault (Figure 12).

Minor faulting occurs within Pleistocene sediment near the Maacama fault; however, these faults have outcrop scale displacements and are considered to have a negligible effect on the sedimentation rate estimates. For instance, the outcrop illustrated in Figure 10 is situated over 100 m west of the Maacama fault and contains late Pleistocene clay and silt offset as much as 70 cm. Another outcrop 4 m from the location of the Thermal Canyon ash (site T, Figure 8A) contains offset beds with greater than 3 m of displacement. Such faulting produces small offsets (< 10 m) and is only prominent near the Maacama fault zone.

Slip Rate of Maacama Fault Inferred from Tephrochronology

A slip rate for the Maacama fault can be calculated by measuring offset tephra units of known age. Several assumptions must be made in order to calculate a slip rate. First, I assume that the Maacama fault has been active since the Thermal Canyon tephra was deposited at ~ 740 ka. Second, I assume that the sedimentation rate in LLV has been relatively constant between 110 ka and 740 ka (time span of tephra deposition). Third, I assume that the unnamed 110 ka tephra found in the geotechnical trench (site S, Figure 8A) is on the east side of the fault zone. I also assume, for all three tephras, that they were deposited, buried and tilted such that if they were completely exposed at the ground surface their outcrop pattern would be linear and depict the approximate east-west strike (and shallow northward dip) of the Pleistocene section. This estimate represents a minimum slip-rate because the Safeway tephra is located in a flower-shaped structure in the Maacama fault-zone. Lateral displacement of the ash deposit may exceed displacement observed in the fault because shear occurs over a zone up to tens of meters wide allowing packages of sediment to become stranded.

Using displaced late Pleistocene tephras in LLV, I infer that the Maacama fault slip rate since the late Pleistocene is of the same order of magnitude as the measured creep rate of the last few decades. Using the conclusion from the sedimentation rate calculation that the unnamed 110 ka ash was deposited on the east side of the fault and the sedimentation rate since deposition of the ~740 ky Thermal Canyon tephra is ~ 1.1 m/ky, the Thermal Canyon tephra was projected from its known position on the west side of the fault at Haehl Creek to its sedimentation-rate-estimated position on the east side of the fault (location of ‘C’ on east side of fault, Figure 12). The Thermal Canyon tephra is interpreted to be displaced approximately 4,000 meters. 4,000 meters divided by the time since deposition (740 ka) gives a displacement rate of ~5 mm/yr for the Haehl Creek site, a rate similar to the 6.6 mm/yr creep rate for the Maacama fault at Willits over the nine year period 1991-2000 (Galehouse, 2002).

The Maacama fault is a dextral strike-slip fault with a possible component of vertical displacement. Well log 110 in cross section G-G’ (Figure 7), located on the eastern side of the Maacama fault reaches Franciscan bedrock rock just over 12 m deep, yet only 250 m to the NW, on the adjacent west side of the Maacama fault, well 94 penetrates 60 m of continental deposits and does not reach Franciscan bedrock. The abrupt change in depth to bedrock may be the result of a component of vertical, east-side-up displacement on the Maacama fault or may be the result of lateral displacement of bedrock topography along the fault zone.

Using sedimentation rate and slip rate estimates, two simple methods can be used to calculate the approximate age of the oldest sediment in LLV. Using the inferred sedimentation rate of 1.1 m/ky and locations of identified tephras, I projected the inferred ages of sediment along the western side of the fault (Figure 12). At the far southern end of the valley the projected age is ~1.1 My (Figure 12).

A second method uses the dip of the basin fill and the location of the most southern (stratigraphically lowest) sediment. Projecting the 8° average dip northward on a longitudinal cross-section from the southern-most bedrock/sediment contact to the North Valley Fault, the oldest sediment is at a depth of 1100 m (Figure 13). Using the calculation of 1.1 m/ky deposition rate and assuming that sediment at the surface is 0 yr, the maximum age of sediment is ~ 1.0 My.

Depositional Facies Observations in Little Lake Valley

Observations of the type and distribution of sediment in LLV create the groundwork for inferring LLV depositional facies. The low hills that occupy southernmost LLV, which are in-part older than 0.74 My (based on tephrochronology), mainly consist of well-rounded to moderately-rounded massive gravel with well-developed imbrication. The gravel is interbedded with planar and trough-cross bedded fine and coarse grained sand. Deposits on the west side of the Maacama fault in southern LLV have sub-rounded gravels as large as 60 cm.

Based on well logs and field investigations, coarse units such as gravel and sand dominate the sediment at the southern end of the valley (bottom of the stratigraphic section) and fine units become more abundant in the central and northern parts of the valley (middle and top of the stratigraphy). On the basis of well log analysis, I infer that vertical accretion of coarse sand and gravel occurred simultaneously with silt and clay aggradation in strata in the central part of the valley. Well log A2 contains 60 m of gravel interbedded with fine lenses of clay and sand (cross section D-D’, Figure 6). Adjacent Well 32, about 600 m to the northeast, contains almost continuous fine grained (silt/clay) sediment at the same depth as the gravel in well A2. A similar relation is observed 1,200 m to the northwest between well A1 and well 20 in cross-section C-C' (Figures 4 and 6). The juxtaposition of vertically accreted gravel units and vertically accreted fine-grained (silt/clay) units is seen throughout the valley although it is most common in wells in the central region. Based on these observations, and using the sedimentation rate (1.1 m/ky), I infer that some middle Pleistocene LLV channels aggraded in one place in the valley for up to 70,000 years, while fine-grained silt and clay floodplain and backswamp deposits aggraded on adjacent valley bottoms keeping pace with channel aggradation. Assuming drainage reversal had occurred, these thick sequences of units might be deposited by a paleo-lake with coarse shoreline units surrounding fine-grained, lower-energy sand and clay. The paleo-lake would be controlled by hydrologic base-level on the North Valley fault at Outlet Creek.

The stratigraphy near the surface in southern and central LLV contains both coarse and fine material in thinner individual beds (5-10 m thickness). For instance, well log A4 on cross-section G-G' (Figure 7) and well log 55 on cross-section F-F' (Figure 7) contain fine and coarse sediment interlayered every 5-10 m. Therefore, I infer a higher frequency of sediment interfingering in LLV above the basal more massive gravel section.

The character and facies associations of the deposits in LLV resemble those deposited by a mixed load fluvial system with intermediate sinuosity (between strongly braided and strongly meandering) (Einsele, 2000). The channel deposits are mainly gravel and sand, and clay and silt are deposited on the floodplains during flood events. These observations are consistent with two types of depositional systems: a braided channel system with adjacent flood plains or a meandering system with adjacent levee/floodplain complexes.

The degree of roundness and clast size of the gravel suggests the sediment originated distally, and gravel clast characteristics are indicative of high energy fluvial environments that have a large (10^3-10^5 Km^2) drainage basin source area (Einsele, 2000). Currently, streams that flow into LLV are small (10-10^2 Km^2) headwater streams and could not supply enough water to form the high energy rivers that dominated LLV in the middle Pleistocene.

Model for Sedimentation and Drainage Reversal in Little Lake Valley

Sedimentation and drainage evolved as the LLV filled with sediment and progressively tilted northward (Figures 14 and 15). The older fluvial sediments exposed at the railroad cut at the southern end of the valley (Figure 12), indicates a high energy environment (Figure 9). Using the method for calculating the age of sedimentation in LLV (Figure 13), I calculated the age of the railroad cut outcrop to be ~ 960 ky. The environment at the time these gravels were deposited may have been a valley-wide braid plain with overbank fine-grained sediment deposited as lenses on the braid plain (Figure 14A).

During deposition in the middle Pleistocene, the region began to undergo northward tilting, which reduced the gradient of streams flowing south through LLV, effectively promoting deposition of more finer material in the valley (Figures 14B and 15). Based on the well log stratigraphy in the central part of the LLV, I infer that in the middle Pleistocene, there was an emerging lower energy environment with geographically confined meanderbelts with coarse sediment deposited in the channel and fairly continuous fine grain deposition on the adjacent floodplains (Einsele, 2000). Such stratigraphy, consisting of thick units that accreted vertically in one location, is characteristic of tectonically subsiding valleys (Einsele, 2000) and is consistent with the inferred progressive northward tilt of the LLV over the course of the Pleistocene (Figure 15). The transition from a presumably more high gradient braided system (Figure 14A) to a more low gradient meandering system (Figure 14B) occurred over a long period of time (hundreds of thousands of years) sometime after the deposition of the Thermal Canyon ash (740 ka).

During the middle to late Pleistocene, minor fan accretion was occurring near the flanks of the valley (Figure 14). Most of the valley contained sluggish, poorly drained backwater and flood plains, and colluvium eroding from the hanging wall of the steeply dipping East Valley fault (Figure 14) deposited fine grained fans that interfingered with the fine fluvial sediment on the valley margins (Figure 14). For instance, the fine grained sediment in wells 26 and 37 of cross section C-C’ (Figure 6) may have been part of a proximal fan delta (as described by Einsele (2000) that was deposited sub-aqueously in a small shallow valley-margin lake.

During the late Pleistocene, northward tectonic tilt and continued north-side-up displacement on the North Valley fault caused drainage reversal and the termination of fluvial input into LLV from the north (Figures 14C and 15). From the late Pleistocene onward, only fine sediment was deposited (sand, and gravel was deposited in small streams throughout LLV). The upward transition to the “fine unit” on cross-section C-C’ (Figure 6) documents the upward textural transition from coarse to fine sediment in the latest Pleistocene. After drainage reversal occurred, Outlet Creek became the outlet to the north for LLV. LLV may have been a closed basin for a short period of time before northward drainage through Outlet Creek, which would have resulted in a valley-wide lake.

On the basis of the above observations, I infer that LLV once contained a through-going river fed from the north end and exiting the valley at the south end but that the south-flowing drainage was defeated by northward tectonic tilt and LLV drainage reversed to north flowing. The former valley outlet to the south is currently a low divide between the LLV (Eel River drainage) and the Ukiah Valley (Russian River) drainage (Figure 2). Evidence for former fluvial connectivity between the Ukiah basin and southern LLV is the similarity of sediments and stratigraphy between the upper stratigraphic units in the Ukiah basin and sediments in southern LLV. Based on field reconnaissance and well log research, stratigraphy is similar in both valleys on the basis of texture, clast size, degree of weathering, frequency and distribution of deposits, and clast lithology.

Tectonic Evolution of Little Lake Valley and Driving Mechanisms for Deformation

Tectonic processes profoundly influenced the landscape evolution and drainage changes in LLV. Pleistocene deposition in LLV was occurring simultaneously with northward valley tilt, and subsidence and tilt was accommodated by motion along both the North Valley fault (up to the north and northwest) and the East Valley fault (up to the east and northeast). Several landforms and deposits testify that northward tilt accommodated on the North Valley and East Valley faults caused drainage reversal. First, an abandoned, north-tilted valley that widens to the south trends southward toward the North Valley fault and LLV (Figure16A). I infer the abandoned valley once accommodated a stream flowing to the south even though the gradient of the tilted valley is now to the north. This valley may be the dissected, eroded paleo-river valley that once contained a river that flowed south into LLV and on to the Russian River via Ukiah basin. The abandoned north-tilted valley is beheaded by the North Valley fault (Figure 16A), which presumably is the structure accommodating northward tilt of the valley.

Additional evidence for uplift north and west of the North Valley fault and subsidence south of the North Valley fault are the uplifted “airport gravels” west of the fault (Figures 3 and 16B). I infer that the airport gravels northwest of LLV were deposited during the early stages of aggradation in LLV and then were vertically displaced up by the North Valley fault, making inception of fault movement a bit younger than the oldest gravel of the LLV basin fill. A fault line scarp of the North Valley fault is apparent along the northwest side of the valley where the airport gravels are preserved (Figure 3), but the North Valley fault is buried by valley fill at the northern end of LLV because the paleo-river that entered LLV from the north eroded the fault scarp making the presence of a fault only apparent in well logs (Figures 4 and 5).

Another possible example of valley margin faulting is Rocktree Valley, located east of LLV 200 m above the valley floor (Figure 4). Rocktree Valley drains to the east-northeast away from LLV, has a valley that widens to the west-southwest toward LLV before the wide valley is abruptly beheaded by the East Valley fault (Figure 4). I infer that Rocktree Valley originally flowed west into LLV and joined the generally south flowing paleo drainage out of LLV. Fault displacement up to the north and east on the East Valley fault tilted the Rocktree valley to the east, eventually defeating the west-flowing Rocktree drainage. The scarp that separates the modern Rocktree Valley from LLV is a fault line scarp of the now inactive East Valley fault.

Northward tilt in Little Lake Valley, accommodated by the North and East Valley faults, continued throughout most of the Pleistocene. Therefore, I infer that the dip magnitude of sediments in LLV decreases in the younger sediments and that lesser dips in younger sediment is accommodated on a series of angular unconformities (Figure 15). Sometime in the late Pleistocene, northward tilt defeated the south-flowing fluvial system and caused drainage reversal; therefore, the Russian/Eel River divide migrated south during the Pleistocene allowing the Eel River drainage to capture previously south-flowing drainages such as those in LLV. The modern divide between the Eel River (LLV) and the Russian River (Ukiah Valley) is currently migrating north leading to imminent recapture by the Russian River of Eel River headwater streams in the upper reaches of Potter Valley and Walker Valley (Figure 17).

The driving mechanism behind the tectonic evolution of LLV is the migration of the Mendocino Triple Junction (MTJ). As the plate boundary to the west changed from a convergent to a strike-slip margin, fold-and-thrust compressional faulting, strike-slip tectonics, and related complex crustal processes all resulted from the evolution of the plate boundary. Paleo basin geometry of LLV may be a product of fold-and-thrust faulting; large synclinal basins to the north such as the Eel River basin were formed by compressional tectonics. If such compression did create a paleo LLV basin, it occurred in the Miocene or Pliocene while the plate boundary to the west was a convergent margin. No geologic evidence of the resulting contraction exists today, so I do not favor that interpretation. Based on subsidence patterns and depositional facies models, crustal extension appears to be the driving mechanism behind LLV basin formation in the Pleistocene.

I infer that generally east-west trending faults accommodate extension in the northern Coast Range by forming a series of basins with north-dipping basin fill (Laytonville basin to the north and Ukiah basin to the south) (Figure 17). The elevation of each basin ascends to the north in a stair step manner (Figure 17). Because basins in the south are lower in elevation, having undergone displacements/rotation for longer periods of time than basins in the north, the schematic north-south trending geologic cross-section of the area from north of LLV to south of LLV (Figure 17) depicts an inferred faulting pattern that closely resembles that of low angle extensional faulting illustrated by Davis and Reynolds (1986). Einsele (2000) illustrates a similar conceptual model of crustal stretching that generates tilted fault blocks bounded by listric faults in the brittle upper crust and ductile creep in the lower crust. In these models, each rotated block would contain sediment tilted in one direction with flat lying Holocene fill at the low end of the valley. Such a scenario is precisely what I observe; the pre-Holocene units in the four major valleys in the cross-section (Figure 17) each have consistently northward dipping stratigraphy (Cardwell, 1964). The timing of extension is unclear but early to mid Pleistocene deposition in LLV may have pre-dated extensional tectonics, while mid to late Pleistocene deposition appears to have occurred syntectonically. Because of the lack of active tectonic features along the North Valley fault and the East Valley fault, I infer that crustal thinning is no longer active in LLV; late Holocene units in LLV are relatively flat-lying, providing evidence that the valley may no longer be undergoing northward tilt.

Patterns of crustal thickening and thinning, following the northward migration of the Gorda slab are predicted by a numerical model of Furlong and Govers (1999). Using this model, extension should have occurred in the LLV in the Pleistocene. Shifts in drainage divide migration direction, as I propose for LLV, also are consistent with proposed geomorphic effects of MTJ migration (Furlong et al., 2003).

CONCLUSIONS

The topography and drainage pattern of the northern Coast Ranges of California formed and evolved largely as a consequence of deformation associated with the migration of the Mendocino Triple Junction. Evaluations of sediment filled basins such as LLV provide a valuable opportunity to analyze Pleistocene deformation.

Field research for this project was conducted in LLV throughout several summers in order to gain a better understanding of Pleistocene basin sedimentation, age control, and the nature of valley geometry. The ages of sediment in LLV have been constrained by tephra identification. The Thermal Canyon tephra (740 ka), found near the bottom of the Pleistocene sediment fill, is the oldest dated sediment in LLV. The Rockland tephra (575 ka) and an unnamed tephra from Clear Lake (110 ka) also have been identified in the valley fill. The Pleistocene sediment has an average bedding dip of 8°, with north-dipping strata throughout the valley. Holocene sediment is presently accumulating from the south-central to the northern end of the valley. In the south-central region, Holocene sediment is up to 9 m thick and is upwards of 30 m thick in the northern end of the valley. Based on clast imbrication data from the Pleistocene alluvium, Pleistocene drainage through the valley was to the south-southeast, opposite to the modern, north-flowing drainage in the valley.

The locations of several dated tephra layers were used to calculate an approximate LLV Pleistocene sedimentation rate of 1.1 m/ky. Employing this sedimentation rate, the approximate age of the oldest basin fill is 1.1 My. Using offset tephra in conjunction with the estimated sedimentation rate, an estimated Maacama fault slip rate for the last ~ 750 ky is ~ 5 mm/yr.

Although silt, sand, and gravel are found throughout the valley fill, the older deposits contain more gravel than the younger deposits. The depositional facies in LLV have evolved simultaneously with northward tilting of the basin, resulting in bedding dips decreasing from older sediment to younger sediment.

Stratigraphy in LLV is consistent with three fluvial facies associations, a braided river system with adjacent floodplains, high energy meandering river system with levees and floodplains and a low energy proximal braided stream with major sediment input from valley margins such as debris flows and alluvial fans. Based on paleoflow data, field observations, and well log observations, LLV once contained a through-going high energy river that flowed through the valley to the south. The river entered the northern end of the valley at the present day site of the head of Outlet Creek and exited the valley to the south into the Russian River. Northward tilting and subsidence, accommodated by motion on the East Valley and North Valley faults, lowered the gradient of the valley and eventually led to drainage reversal; the valley currently drains north into the Eel River through a bedrock sill at outlet creek which controls the hydrologic base level of LLV.

Pleistocene stratigraphy and subsurface geometry of LLV and other nearby basins resembles characteristics of basins formed by extension and crustal thinning. The valley subsidence and tilting in the vicinity of the Eel River/Russian River drainage divide may be the result of crustal thinning occurring as the result of the northwardly migrating MTJ.

REFERENCES CITED

Atwater, T., 1970, Implications for plate tectonics for the Cenozoic tectonic evolution of western North America, Geological Society of America Bulletin, v. 81. p.3513-3535.

California Department of Water Resources, 1956, Geology, hydrology and water quality of alluviated areas in Mendocino County and recommended standards of water well construction and sealing, Water Quality Investigations Report No. 10, 211 p.

Cardwell, G.T., 1965, Geology and ground water in Russian River valley areas and in Round, Laytonville, and Little Lake Valleys, Sonoma and Mendocino Counties, California, U.S. Geological Survey Water-Supply Paper 1548, 154 p.

Davis, G.H. and Reynolds, S.J,. 1996, Structural Geology of Rocks and Regions, John Wiley and Sons Publishing, New York, 776 p.

Dickinson, W.R. and Snyder, W.S., 1979, Geometry of triple junctions related to San Andreas transform, Journal of Geophysical Research, v. 84, p. 561-572.

Einsele, G., 2000, Sedimentary Basins: Evolution, Facies, and Sediment Budget, Springer-Verlag, Berlin, 792 p.

Fenton, C.H., Prentice, C.S., Benton, J.L., Crosby, C.J., Sickler, R.R., and Stephens, T.A. 2002, Paleoseismic Evidence for Prehistoric Earthquakes on the Northern Maacama Fault, Willits, California. EOS Trans. AGU, v. 83(47), Fall Meeting abstract S11B-1143.

Fox, K.F., 1983, Tectonic setting of the late Miocene, Pliocene, and Pleistocene rocks in part of the Coast Ranges north of San Francisco, California, U.S. Geological Survey Professional Paper 1239, 33 p.

Fox, K.F., Fleck, R.J., Curtis, G.H. and Meyer, C.E., 1985, Implications of the northwestwardly younger age of the volcanic rocks of west-central California, Geological Society of America Bulletin, v. 96, p. 647-654.

Freymueller, J.T., Murray, M.H., Segall, P., and Castillo, D. 1999, Kinematics of the Pacific-North American plate boundary zone, northern California, Journal of Geophysical Research, v. 104, p. 7419-7442.

Furlong, K. P., and Govers, R., 1999, Ephemeral crustal thickening at a triple junction: the Mendocino crustal conveyor: Geology, 27, 127-130.

Furlong, K.P., Lock, J., Guzofski, C., Whitlock, J. and Benz, H., 2003, The Mendocino crustal conveyor: making and breaking the California crust, International Geology Review, v. 45, p. 767-779.

Furlong, K.P. and Schwartz, S.Y., 2004, Influence of the Mendocino Triple Junction on the tectonics of coastal California, Annual Review Earth Planetary Science, v. 32, p. 403-433.

Galehouse, J.S., 2002, Data from Theodolite Measurements of Creep Rates on San Francisco Bay Region Faults, California: 1979-2001, USGS Open-File Report 02-225.

Graham, S.A. and Dickinson, W.R., 1978, Evidence for 115 kilometers of right slip on the San Gregorio-Hosgri fault trend, Science, v. 199, p. 179-181.

Jennings, C.W. and Strand, R.G., 1960, Geologic Map of California, Ukiah Sheet, California Division of Mines and Geology, 1:250,000.

Kelsey, H.M. and Carver, G.A., 1988, Late Neogene and Quaternary tectonics associated with the northward growth of the San Andreas transform fault, Northern California, Journal of Geophysical Research. v. 93, p. 4797-4819.

Lanphere, M.A., Champion, D.E., Clynne, M.A., and Muffler, L.J.P., 1999, Revised age of the Rockland tephra, northern California: implications for climate and stratigraphic reconstructions in the western United States, Geology, v. 27, p. 135-138.

McLaughlin, R.J., 1978, Preliminary geologic map and structural sections of the central Mayacamas Mountains and the Geysers steam field, Sonoma, Lake, and Mendocino Counties. U.S. Geological Survey Open-File Map 78-389. Scale 1:24,000, two sheets.

McLaughlin, R.J., 1981, Tectonic setting of pre-Tertiary rocks and its relation to geothermal resources in the Geysers-Clear Lake area, U.S. Geological Survey Professional Paper 1141, p. 3-23.

McLaughlin, R.J. and Nilsen, T.H., 1982, Neogene non-marine sedimentation and tectonics in small pull-apart basins of the San Andreas fault system, Sonoma County, California, Sedimentology, v.29, p. 856-876.

Merritts, D. and Bull, W.B., 1989, Interpreting Quaternary uplift rates at the Mendocino triple junction, Northern California, from uplifted marine terraces, Geology, v. 17, p. 1020-1024.

Meyer, C.E., Sarna-Wojcicki, A.M., Hillhouse, J.W., Woodward, M.J., Slate, J.L., and Sorg, D.H., 1991, Fission-track age (400,000 yr) of the Rockland tephra based on inclusion of zircon grains lacking fossil fission tracks, Quaternary Research, v. 35, p. 367-382.

Nilsen, T.H. and McLaughlin, R.J., (1985) Comparison of tectonic framework and depositional patterns of the Hornelen strike-slip basin of Norway and the Ridge and Little Sulfur Creek strike-slip basins of California, The Society of Economic Paleontologists and Mineralogists, Special Publication No 37, p. 79-103.

Pampeyan, E.H., Harsh, P.W., and Coakley, J.M., 1981, Preliminary map showing recently active breaks along the Maacama fault zone between Laytonville and Hopland, Mendocino County, California, U. S. Geological Survey Map MF-1217, scale:1:24,000.

Sarna-Wojcicki, A.M., Meyer, C.E., Bowman, H.R., Hall, N.T., Russel, P.C., Woodward, M.J. and slate, J.L. 1985, Correlation of the Rockland ash bed, a 400,000-year-old Stratigraphic marker in northern California and western Nevada, and implications for middle Pleistocene paleogeography of central California, Quaternary Research, v. 23, p. 236-257.

Sarna-Wojcicki, A.M., Meyer, C.E., Adam, D.P., and Sims, J.D., 1988, Correlations and age estimates of ash beds in late Quaternary sediments of Clear Lake, California, in Late Quaternary Climate, Tectonism and Sedimentation in Clear Lake Northern California, Sims, J. D. (ed.) Geological Society of America Special Paper 214, p. 141-150.

Upp, R.R., 1989, Holocene activity and tectonic setting of the Maacama fault zone, Mendocino County, California, Engineering Geology, v. 27, p. 375-412.

TABLES

Table 1. Radiocarbon ages from sediment of Little Lake Valley.

Sample Name	Date Collected	Sample Material	Laboratory Number	Lab Reported ^{14}C Age with 2-sigma error	Calibrated age range *
03 WH 02	10-03-03	Hardwood Tree Root**	GX-30605-AMS	11570 +/- 60 ^{14}C years BP	Cal BP 13422-13543
03 HC 02	10-10-03	Fabaceae *Lupinus* Seeds***	GX-30606-AMS	15810 +/- 60 ^{14}C years BP	Cal BP 17813-19974

* Calibrated years before AD 1950, using calibration program of Stuiver et al. (1998). Calibration incorporates two standard deviations and an error multiplier of one.
** On the basis of investigation of wood cell structure, John Stuart, HSU Forestry Dept, identified sample as a hardwood species (not conifer), maybe cottonwood or willow.
*** Seed analyzed by Jim Effenberger, California Dept of Food and Agriculture Seed Laboratory. Due to the absence of both the hilum and embryo results mostly were inconclusive but seeds may represent Fabaceae *Lupinus*, or Lupine plant.

Table 2. Identification and age of tephra located in Little Lake Valley sediment.

Site Location	Depositional Environment	Tephra name and origin	Tephra Age	Reference
Downtown Willits, CA 200 m South of Safeway in Maacama Fault Paleoseismic Trench	clayey silt	Unnamed tephra. Correlated to tephra in core from Clear Lake, CA (Sarna-Wojcicki et al. 1988). Source most likely Sierra Nevadas.	110 Ka	This Study, (Sarna-Wojcicki, pers. Comm., August, 2004)
Hwy cut in US 101. 3 km SSE of Willits, CA	Fine grain sand and silt	Rockland ash. Lassen Peak, CA (Mt. Tehama)	575 Ka	Sarna-Wojcicki et al, (1985), Meyer et al, (1991) Lanphere et al, (1999),
Haehl Creek stream bed exposure.	Lignite and silt	Thermal Canyon Ash. Long Valley Caldera, CA	740 Ka	This Study, (Sarna-Wojcicki, pers. Comm, November, 2003)

FIGURES

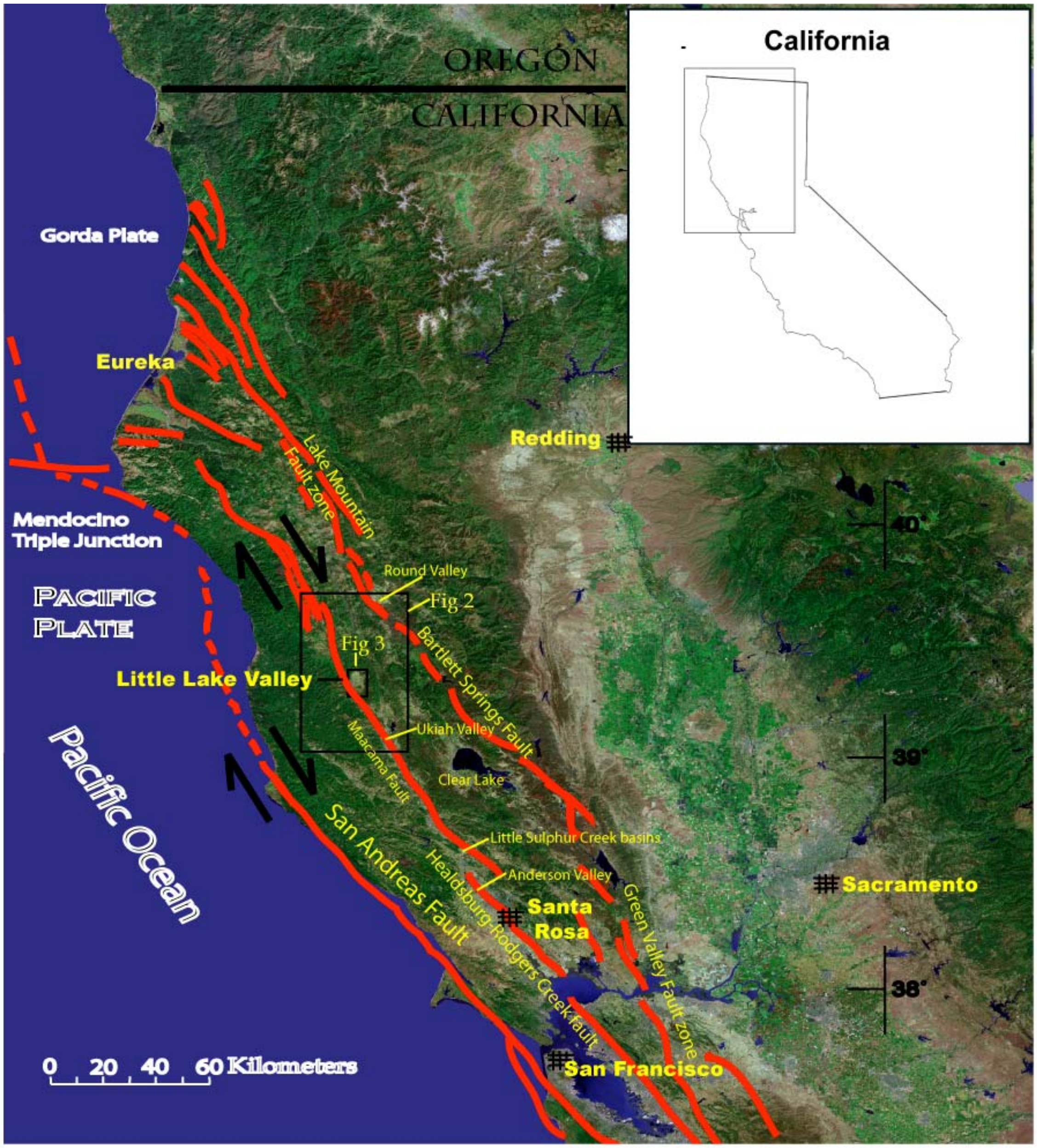

Figure 1. Map of northern California showing study area (small rectangle that is labeled Fig. 3) and principal fault zones.

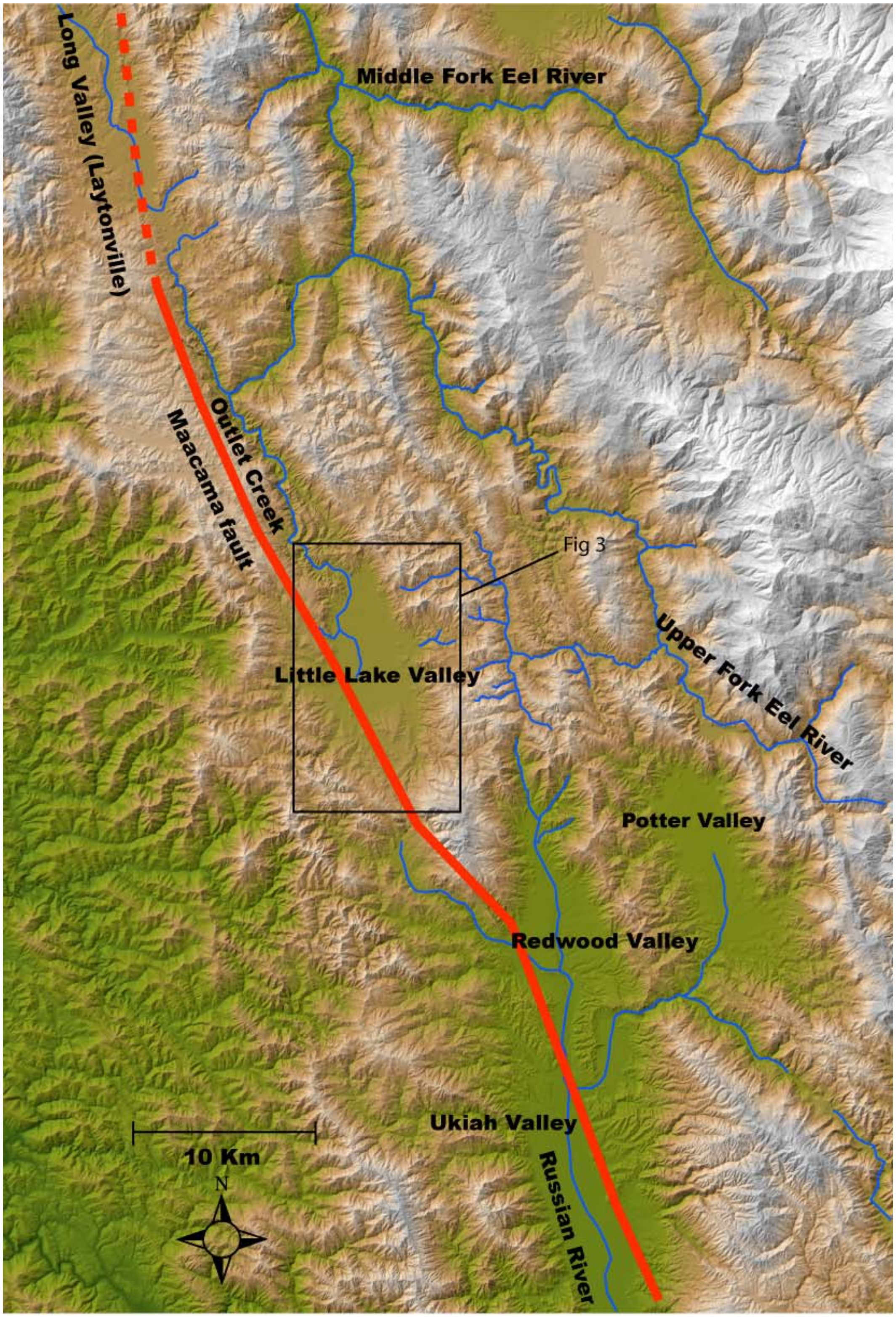

Figure 2. Digital elevation model of a portion of the northern California Coast Ranges showing the Maacama fault zone and major fluvial systems.

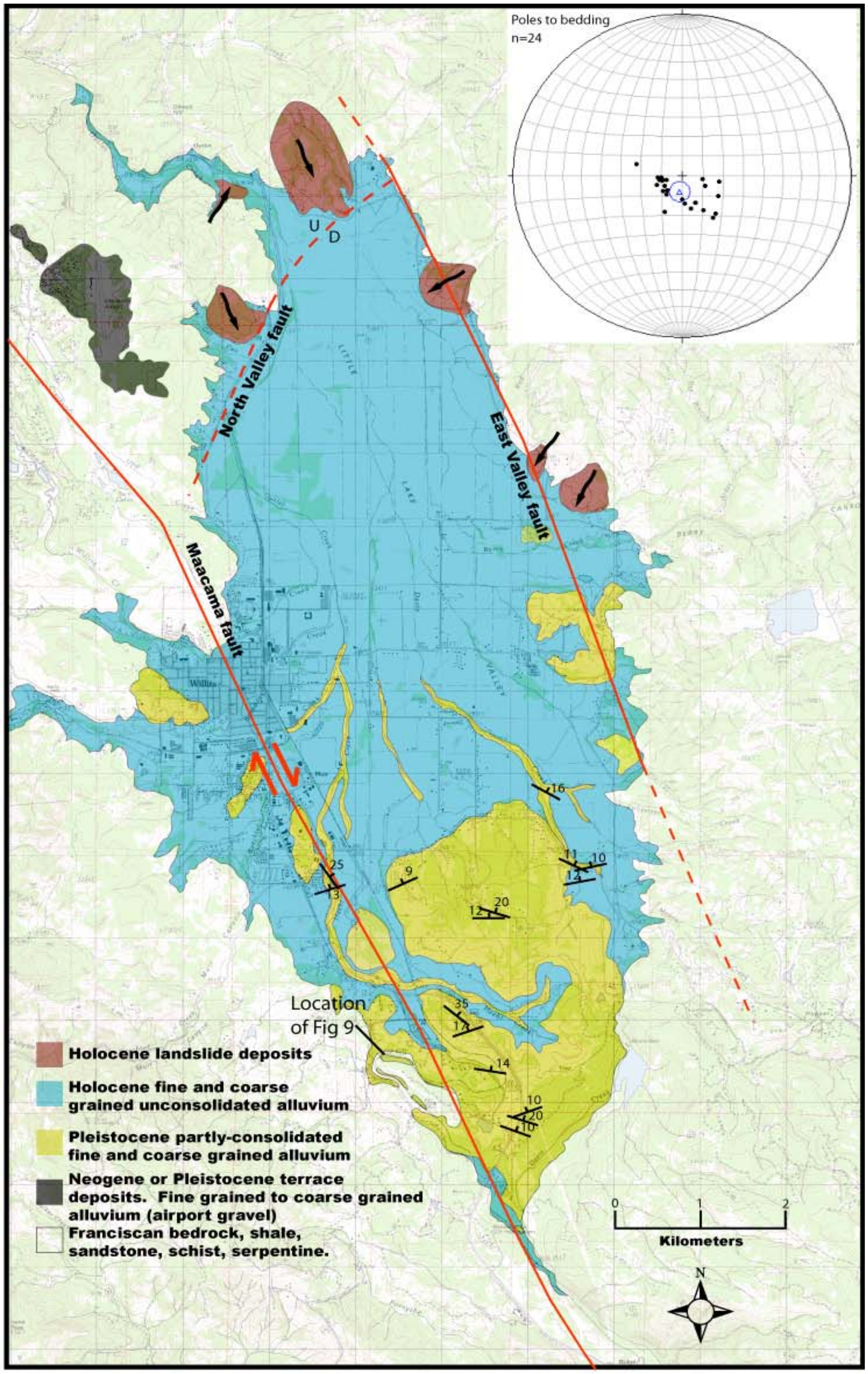

Figure 3. Geologic map of Little Lake Valley. Inset: great circle stereonet of poles to bedding planes for bedding measurements in Pleistocene alluvium of Little Lake Valley.

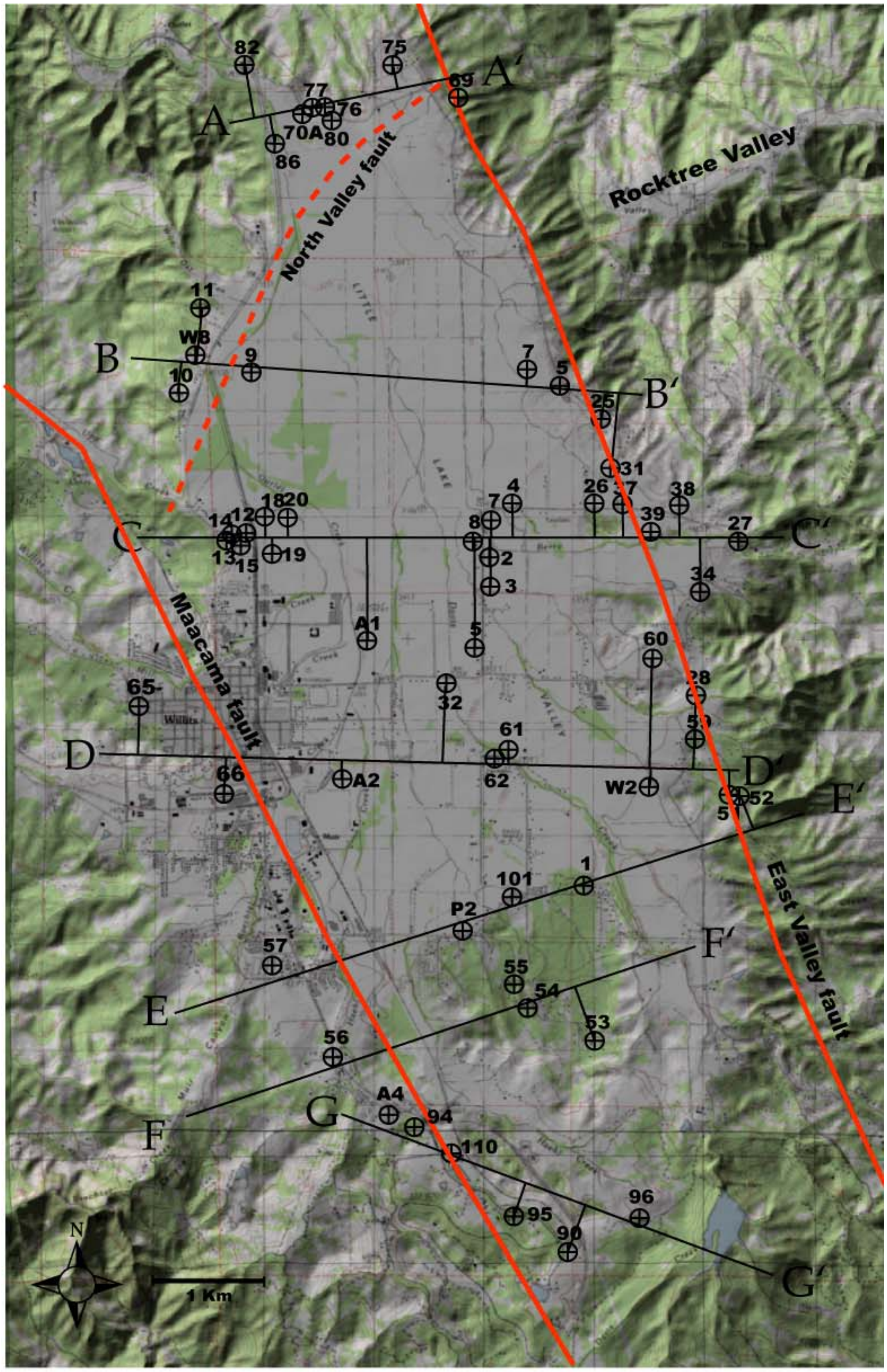

Figure 4. Index map showing locations of well logs in Little Lake Valley and cross section locations.

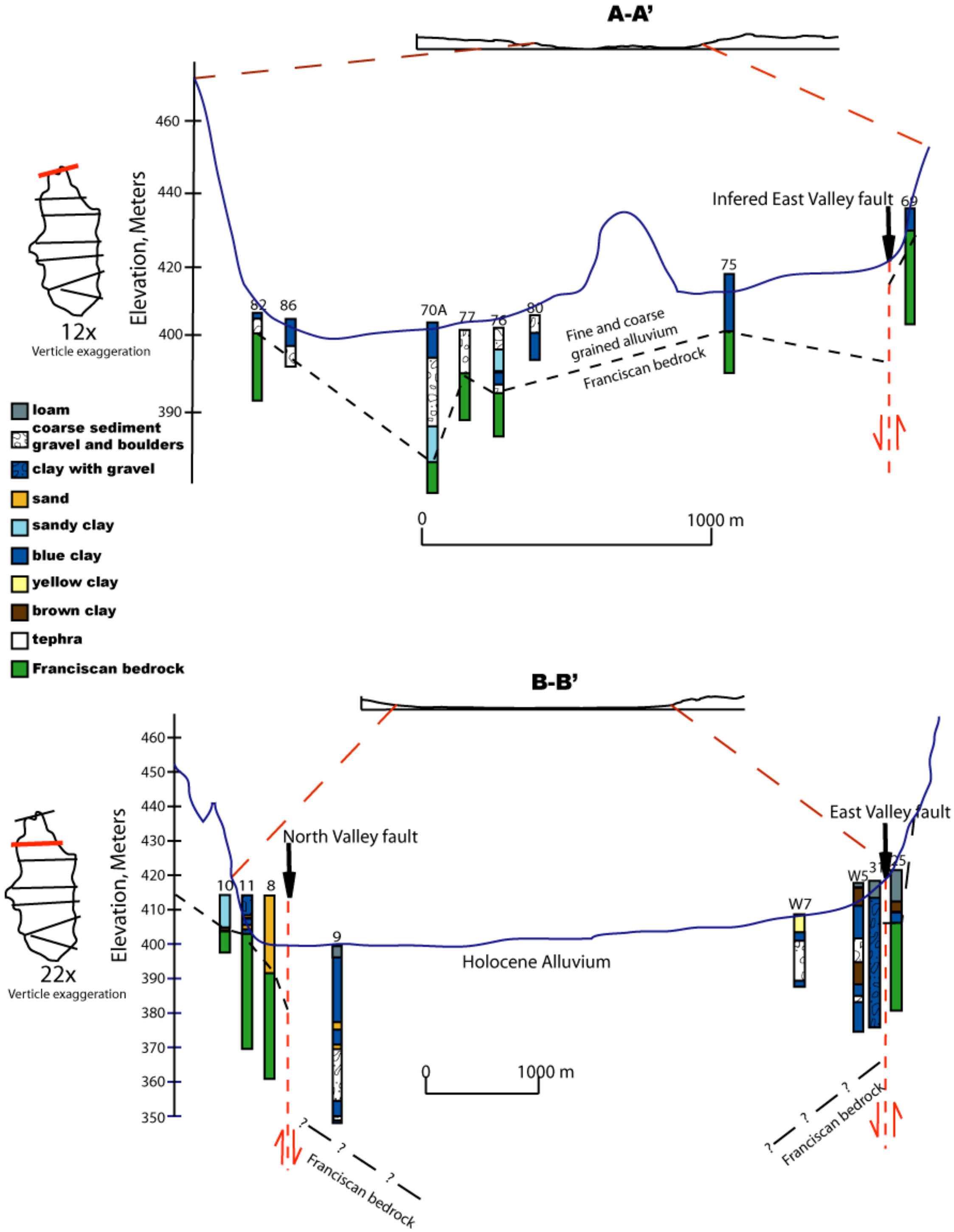

Figure 5. Well log cross sections A-A' and B-B', showing interpretations of Pleistocene sedimentary units.

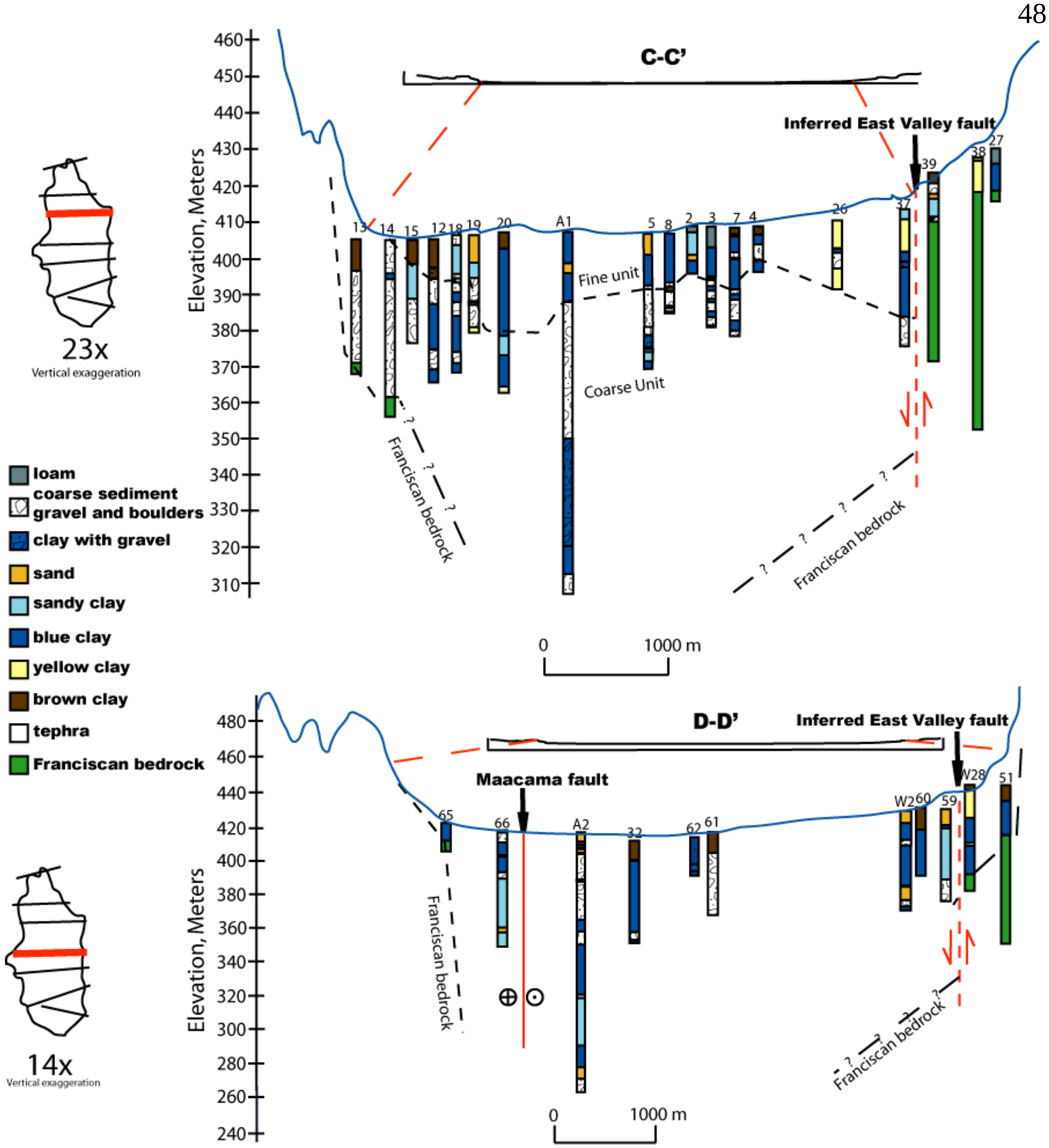

Figure 6. Well log cross sections C-C' and D-D', showing interpretations of Pleistocene sedimentary units.

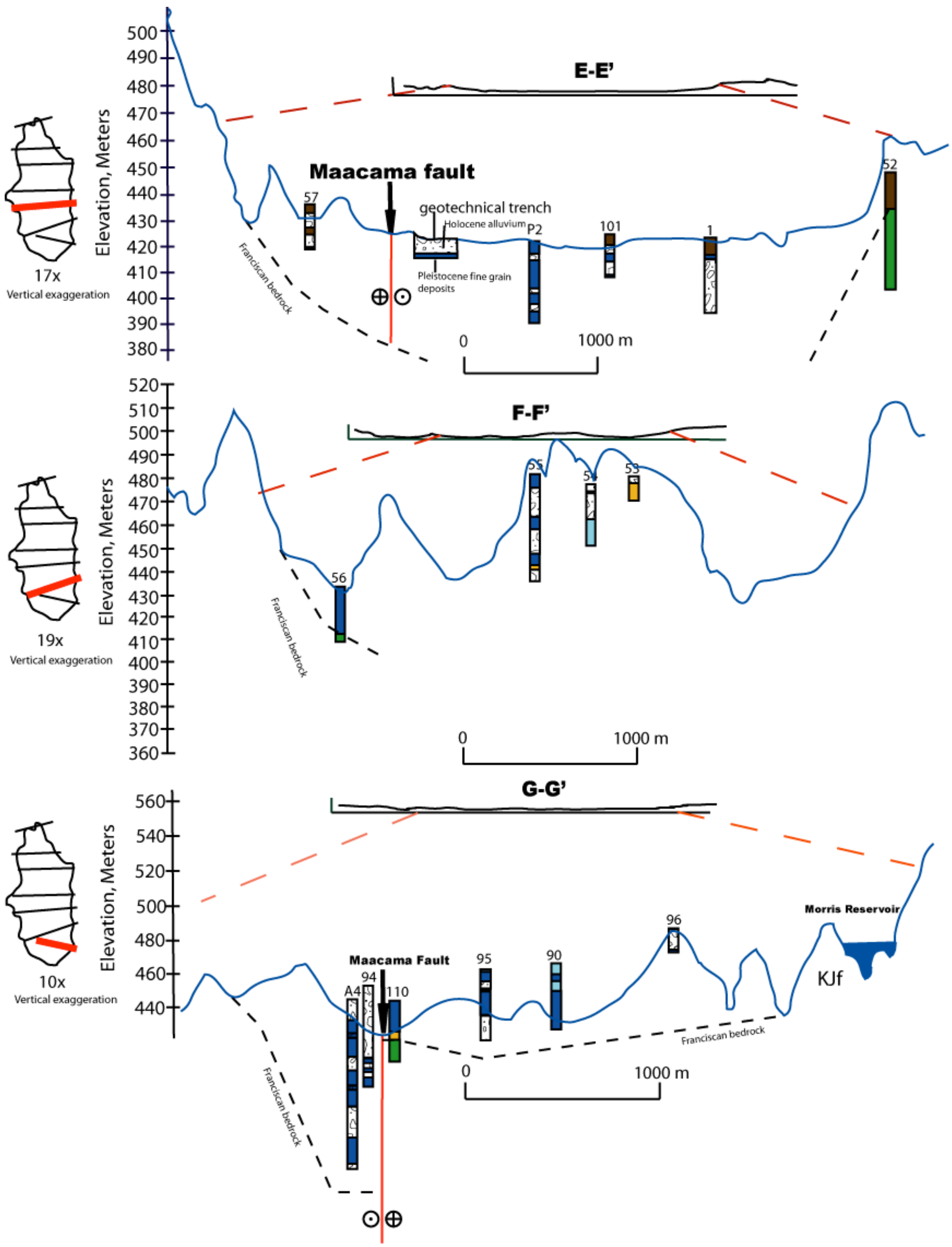

Figure 7. Well log cross sections E-E', F-F' and G-G', showing interpretations of Pleistocene sedimentary units.

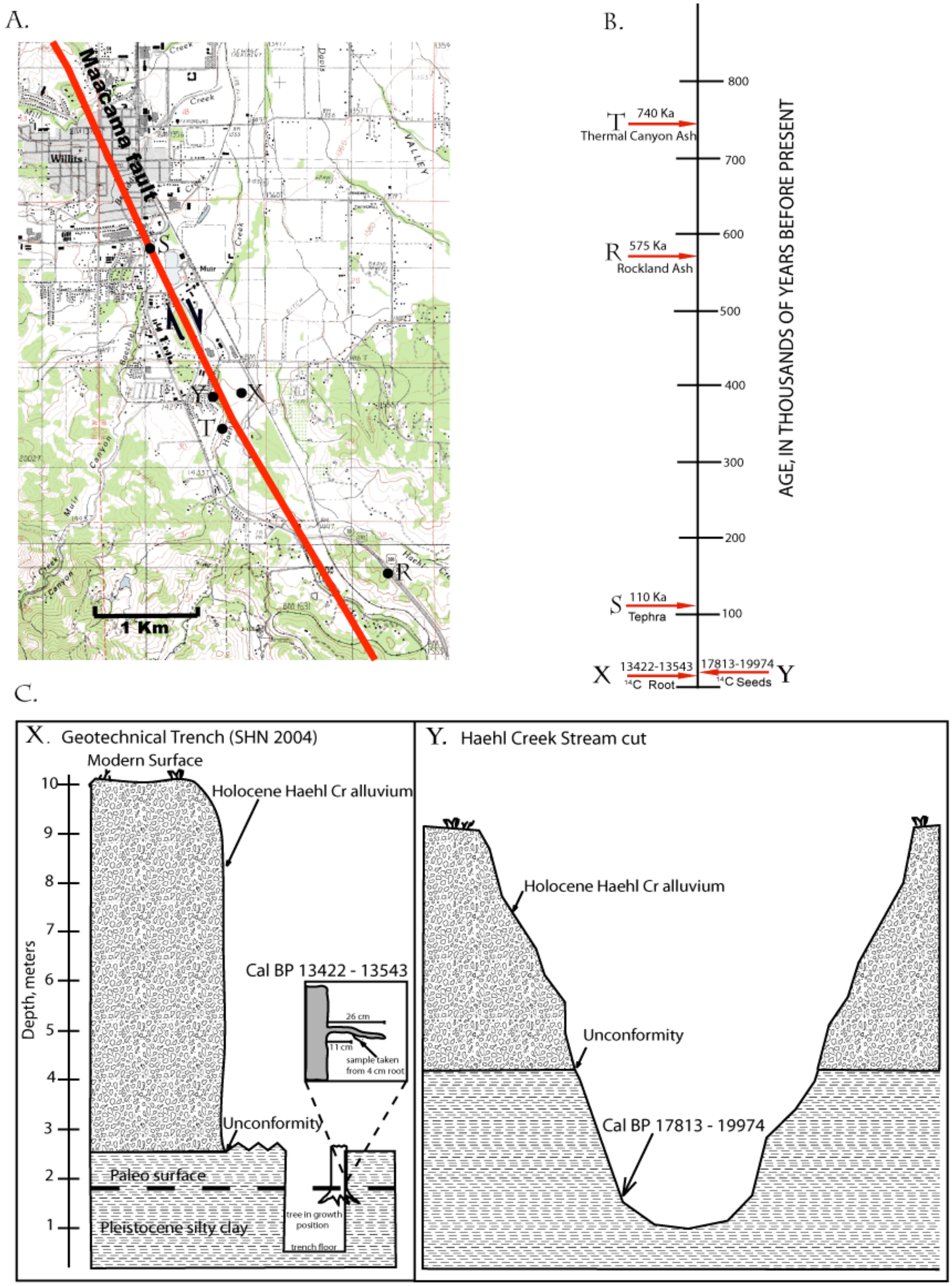

Figure 8. A. Location map of tephra (R, T) and radiocarbon (X, Y) sample localities.
B. Time line of tephra and radiocarbon samples (also see Tables 1 and 2).
C. Schematic geologic cross-sections at sites X and Y showing depth and position of 14C age determinations.

A

B

Figure 9. Photographs of railroad cut outcrop at the south end of the valley (see Fig. 3 for outcrop location). Clasts are poorly sorted and moderately to well rounded. Photographs taken 20 m apart in same exposure.
A. Sub-rounded 60 cm boulder in consolidated fluvial gravel. B. Well rounded 20 cm boulder in consolidated fluvial gravel.

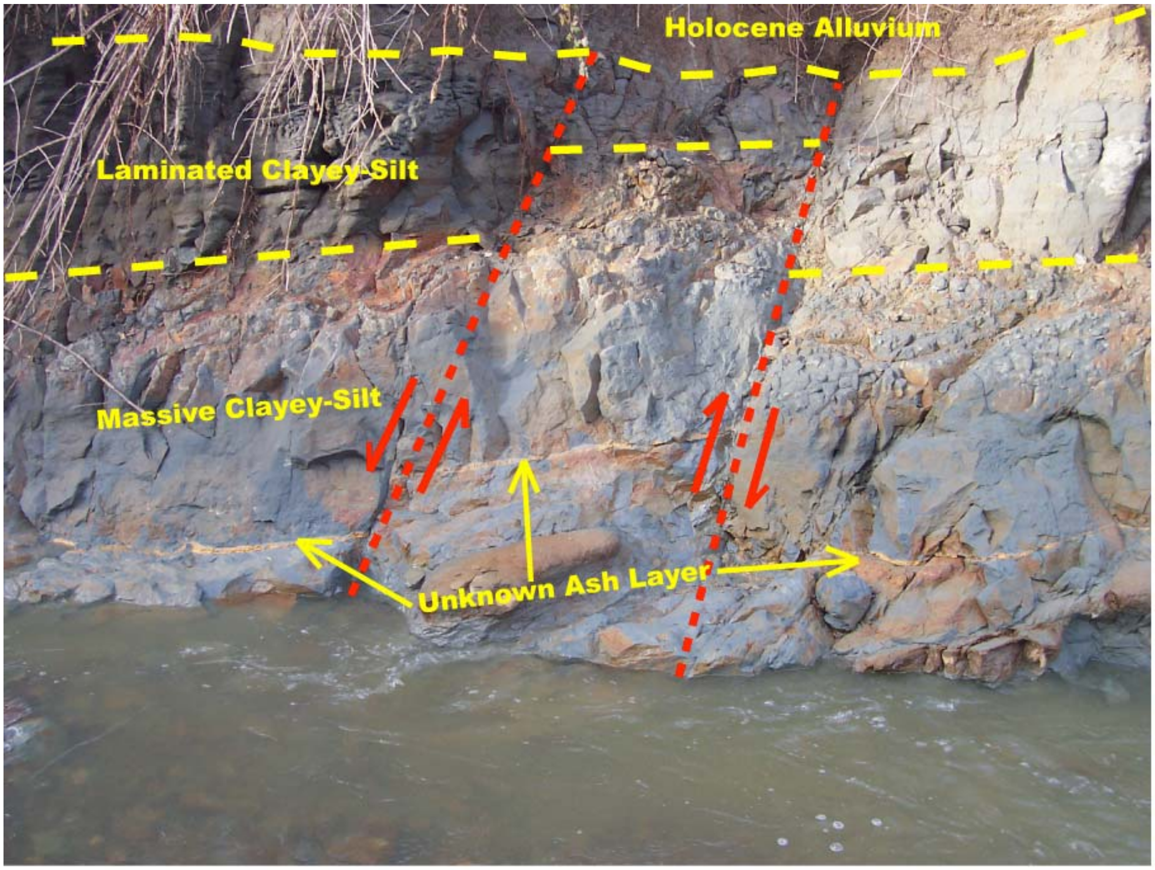

Figure 10. Photograph of outcrop on east bank of Haehl Creek (3 m north of site Y, Fig 8A) showing offset clay and silt units near Maacama fault zone.

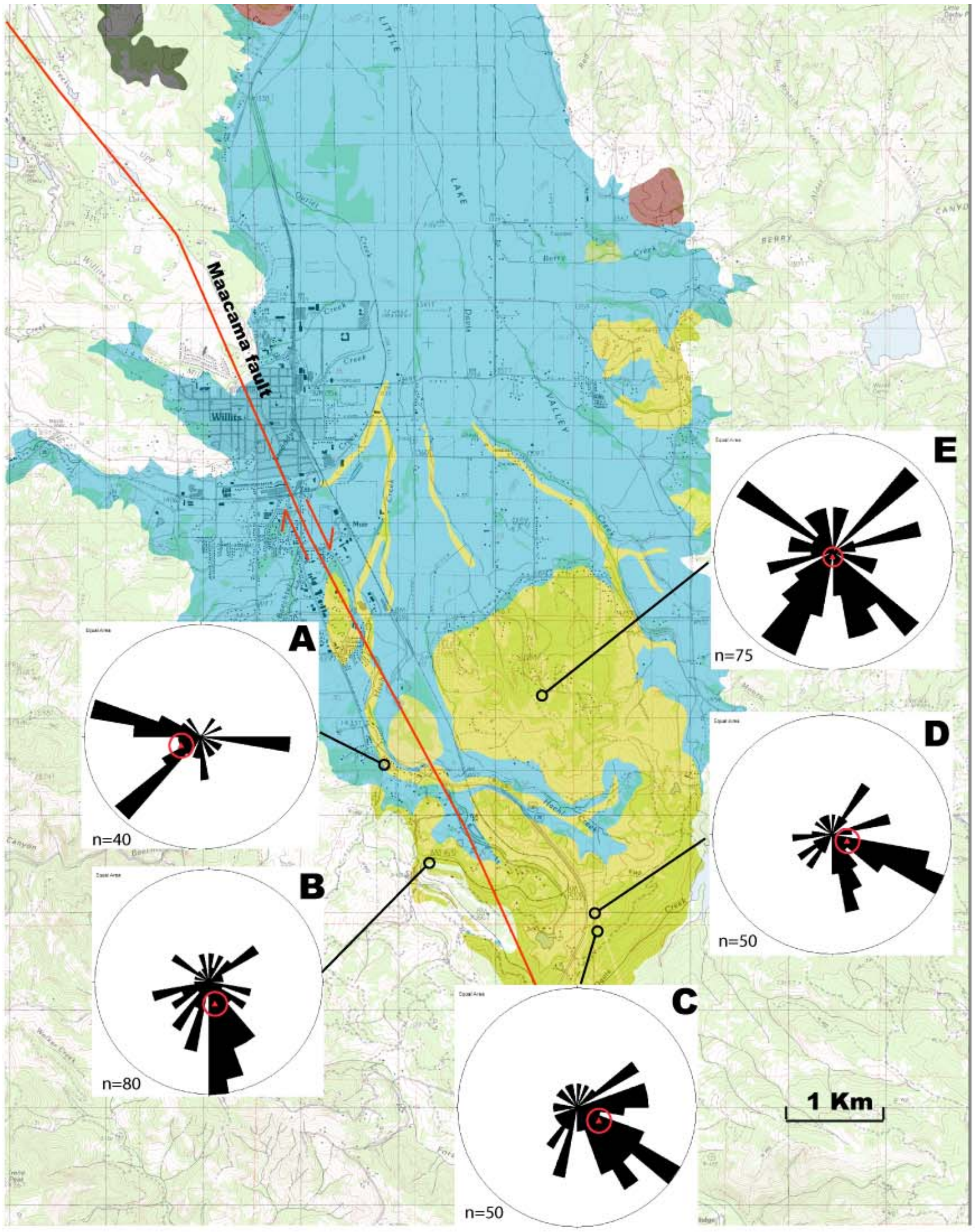

Figure 11. Geologic map of southern Little Lake Valley showing results of clast imbrication measurements at five sites. Red circles indicate mean trend and plunge of clast imbrication, which points in direction of inferred paleoflow.

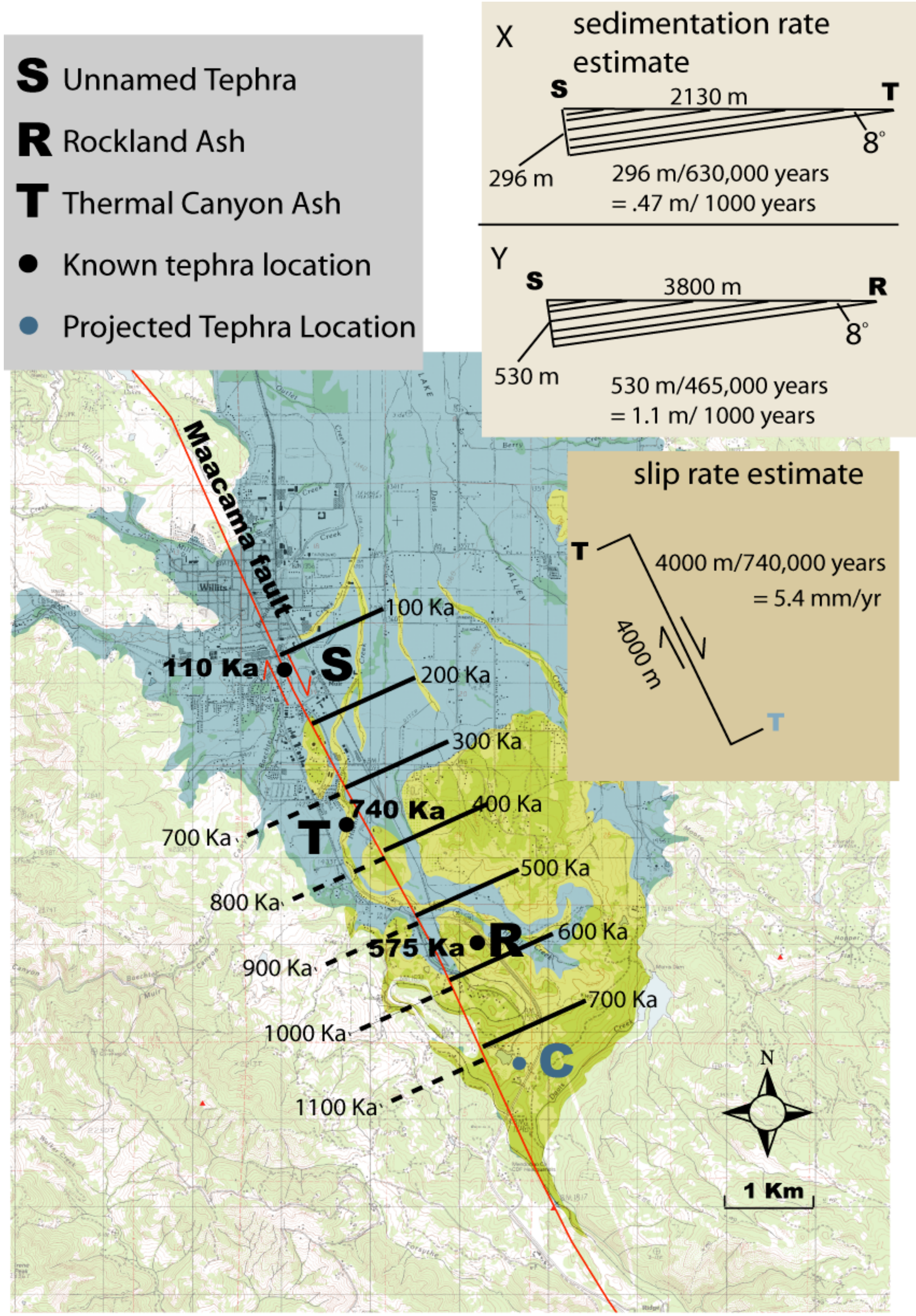

Figure 12. Diagram showing methods of calculating sedimentation rate and slip rate on the Maacama fault. Inset shows calculation for sedimentation rate.

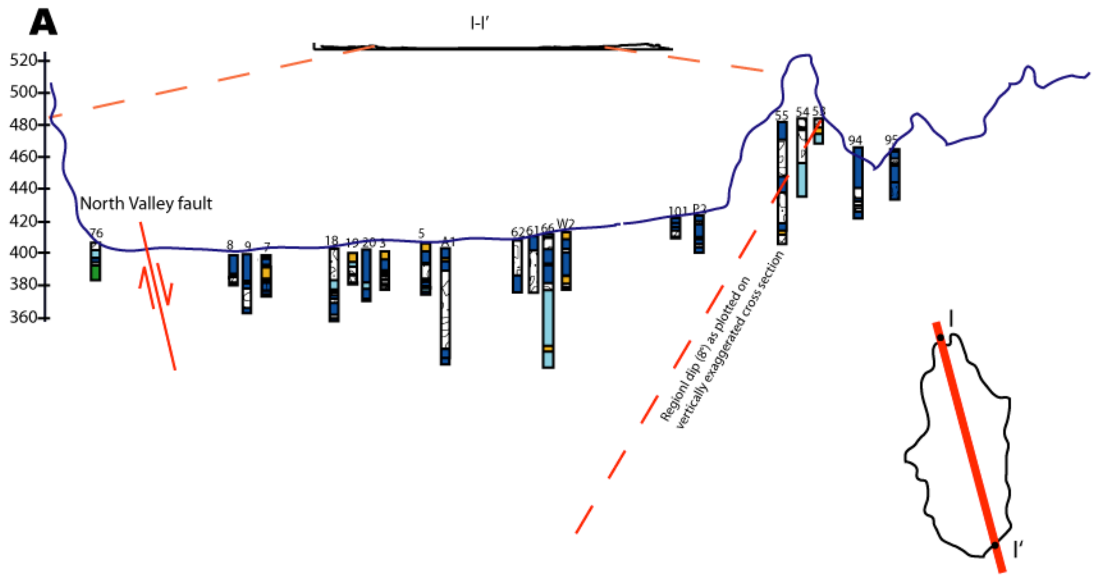

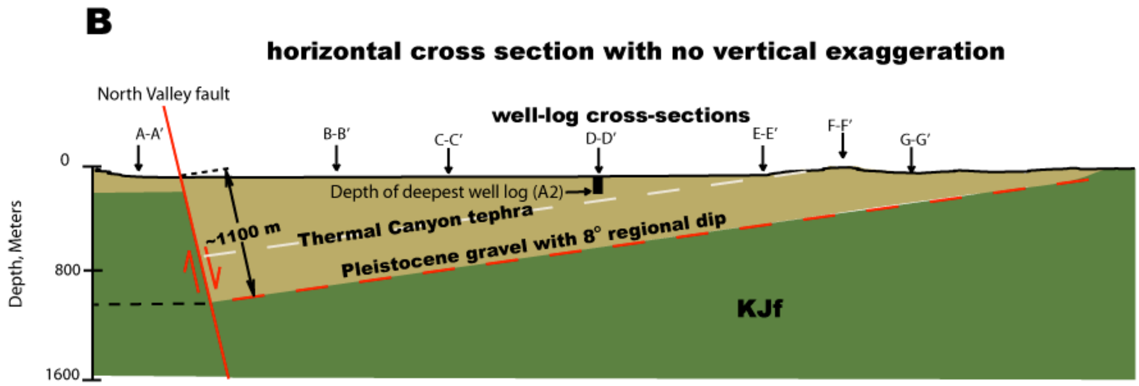

Figure 13. A. Well log cross section I-I' showing interpretations of Pleistocene sedimentary units. Cross section is parallel to long axis of valley. B. Cross section with no vertical exaggeration showing locations of all well log cross sections, depth of deepest well log, inferred stratigraphic position of Thermal Canyon tephra, and inferred minimum thickness of the Pleistocene section.

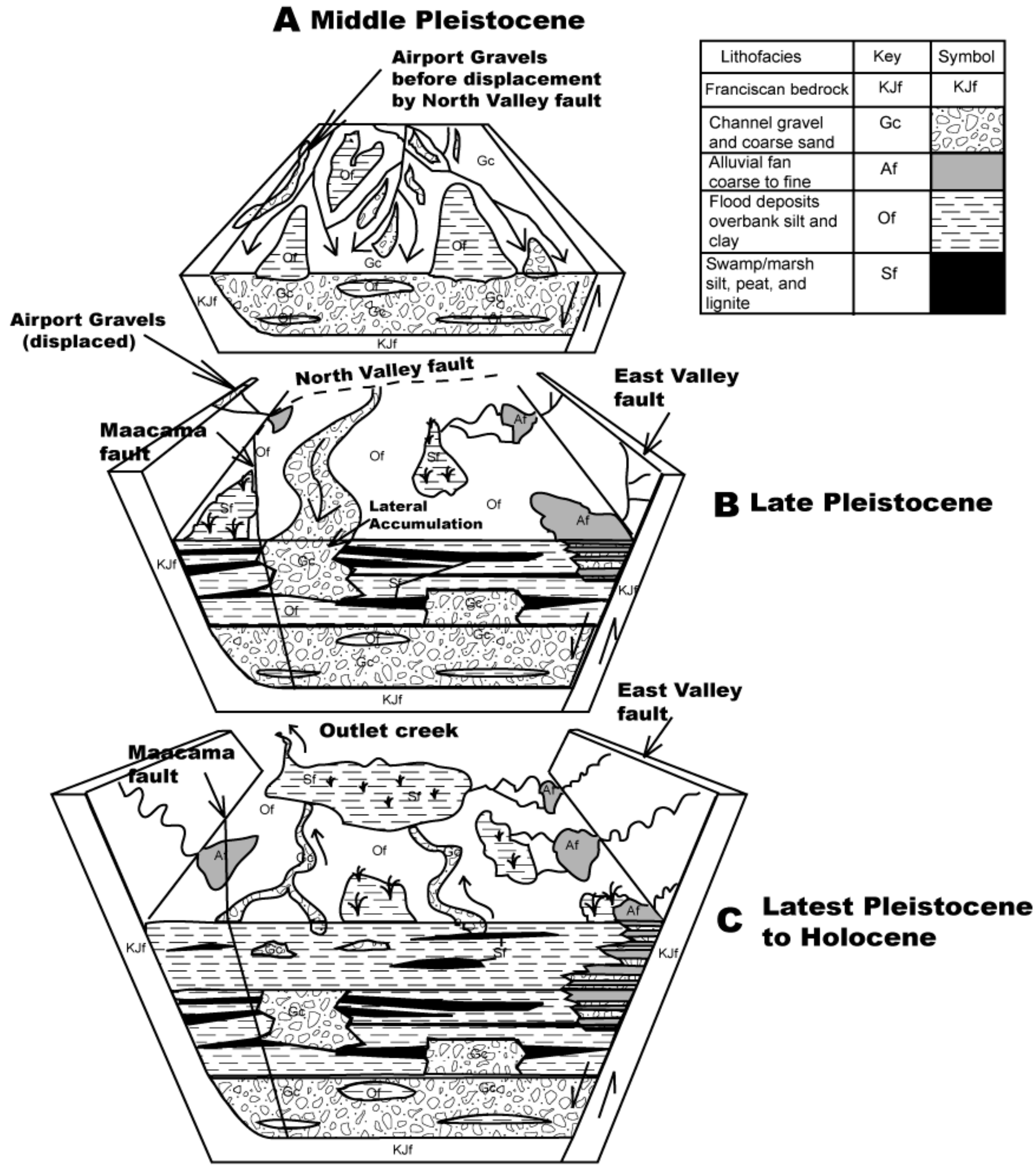

Figure 14. Facies model interpretations through time for Little Lake valley. A. Middle Pleistocene; high gradient, proximal braided river or high energy meandering system; unit are gravel dominated with thick lenses of clay, silt, and sand; sediment source is distal. B. Late Pleistocene; gradient is lowered and sediment and drainage area is decreased; meandering river with adjacent levee/floodplain complexes; gravel is mainly confined to channels by levees; aggradation within channels keeps pace with basin subsidence; accretion of silt/clay on floodplains and in backswamp areas keeps pace with main channel aggradation; sediment is derived from proximal and distal sources. C. Latest Pleistocene to Holocene; low gradient; sand silt and clay dominated; sediment derived from proximal sources such as debris flows, alluvial fans, and seasonal flowing, meandering streams.

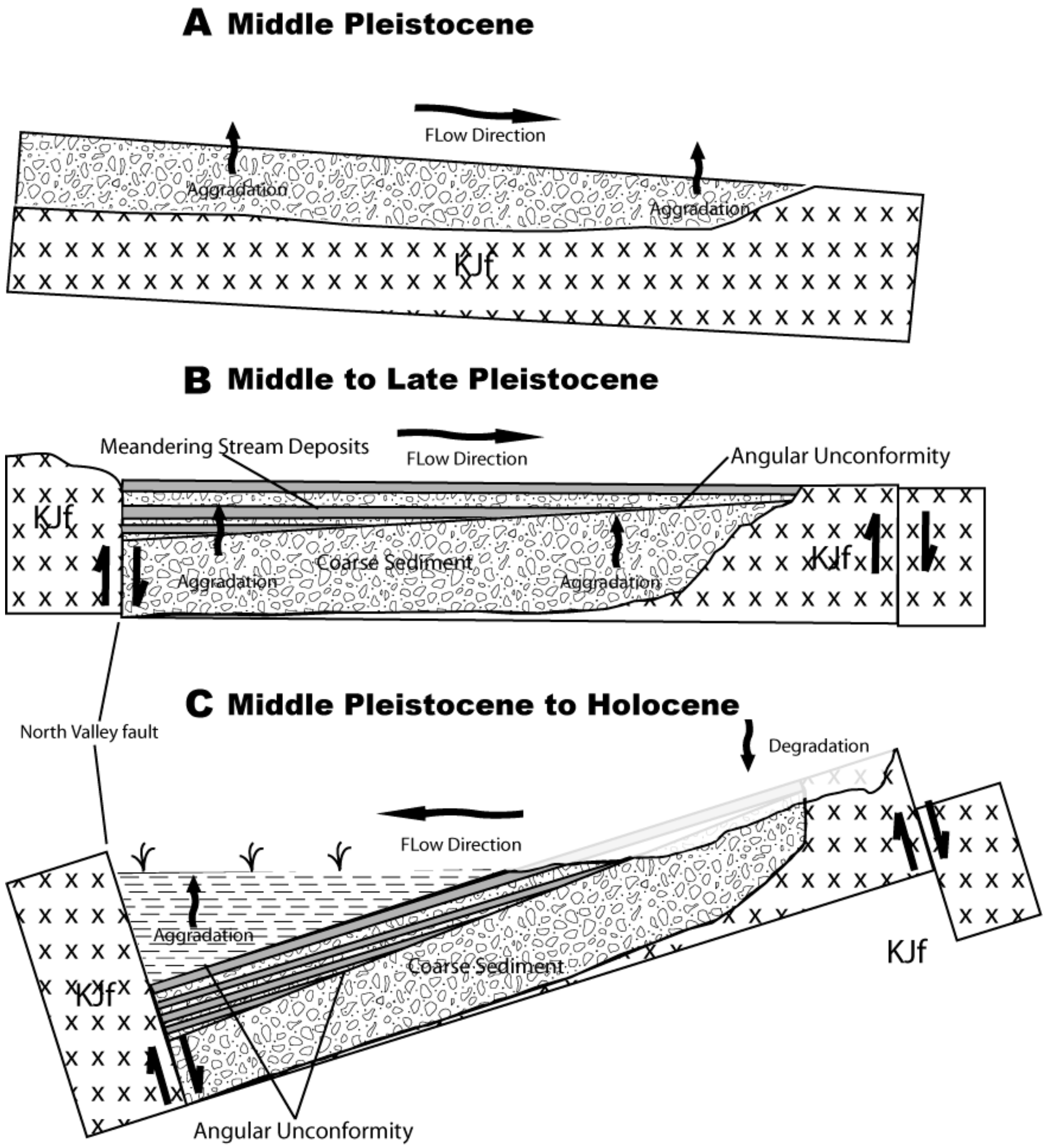

Figure 15. Model of LLV basin tilt showing zones of aggradation and zones of degradation. Tilt is driven by displacement on the North Valley fault.

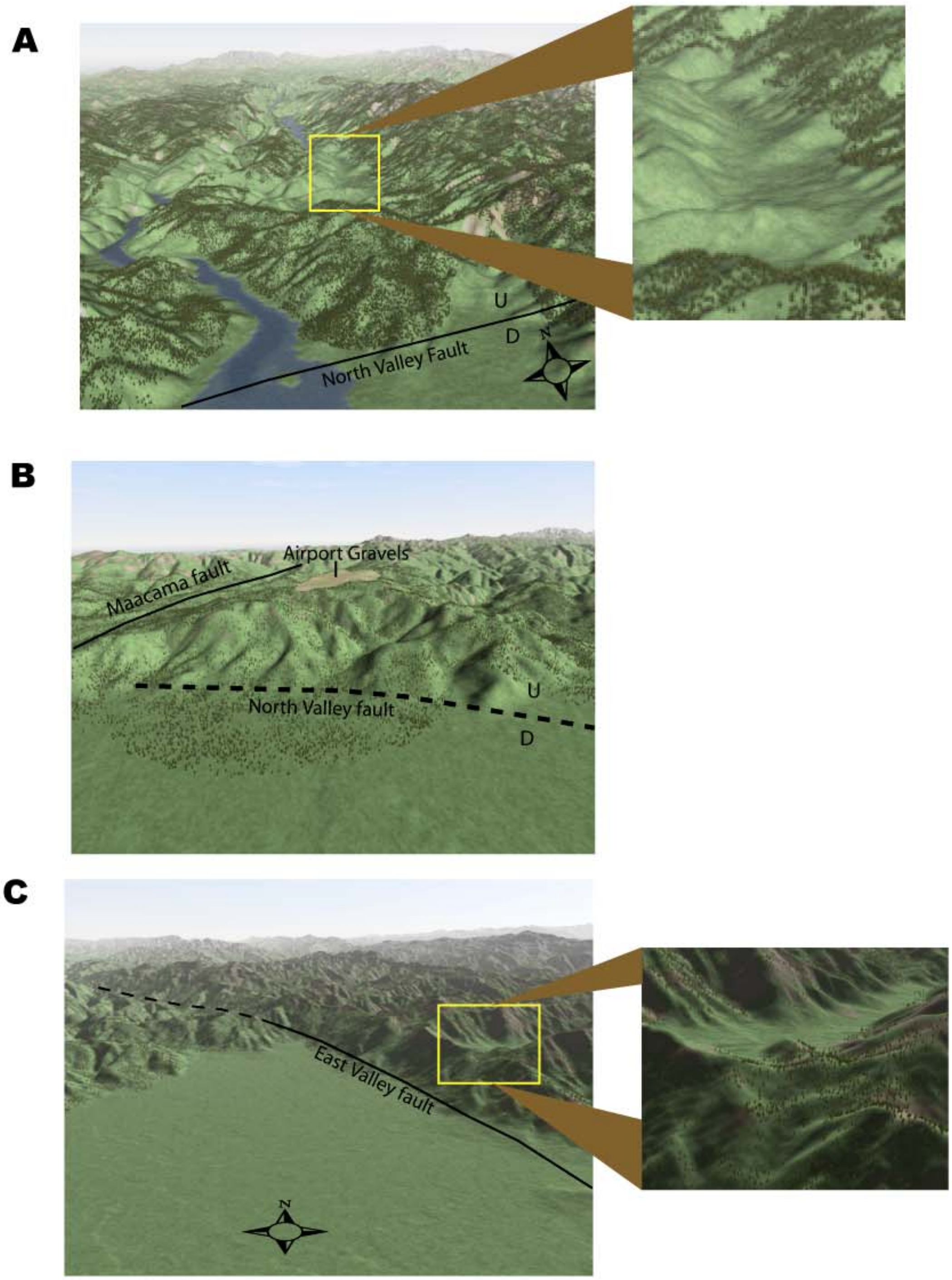

Figure 16. Oblique views of faults in LLV and geomorphic and stratigraphic evidence for vertical offset. A. A wind gap north of LLV showing a channel abandoned by subsidence along the North Valley fault. B. Airport gravels lie 200 m above LLV and may be an uplifted remnant of the LLV basin fill. C. Rocktree Valley, east of East Valley fault, is a gently sloping, wide valley that appears to be offset from the valley floor.

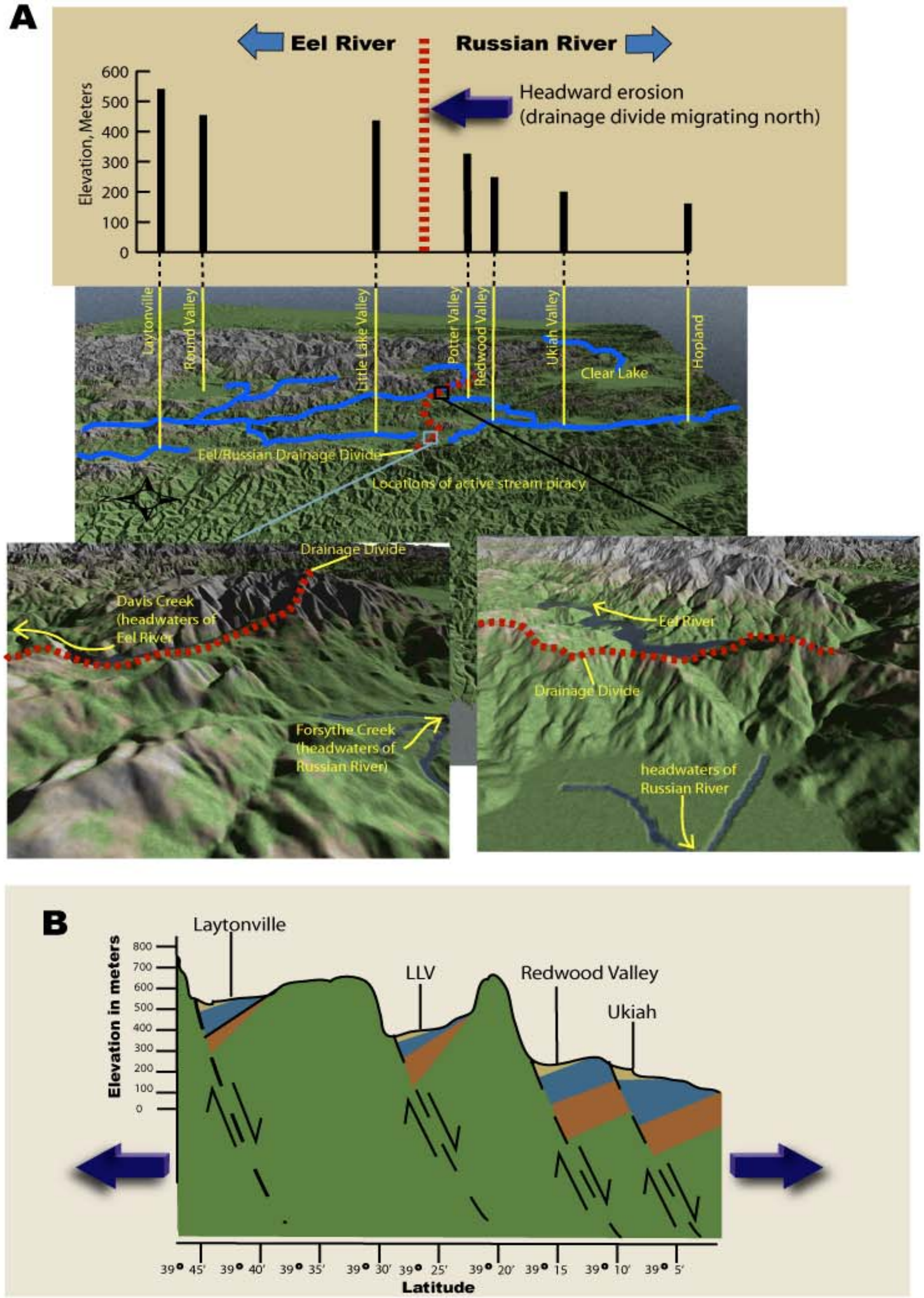

Figure 17. A. Oblique view facing east of major intermontane basins in the northern California Coast Ranges showing major streams and rivers and location of the Eel/Russian River drainage divide. Bar graph depicts mean elevation (in meters) of intermontane valleys going from north to south.
B. Oblique DEM rendering of two areas on the modern Eel/Russian River drainage divide currently undergoing stream piracy. C. Schematic north-south trending geologic cross-section of four major intermontane valleys in the region showing inferred low angle listric faults bounding each valley and separating northward rotated blocks with north-dipping valley fill.